SSP 2022 – Vienna – 2022-09-01

The BASE Experiment

Stefan Erlewein

(Max Planck Institute for Nuclear Physics)

on behalf of the BASE collaboration

Outline

- Introduction
  - Measurement principle
  - The BASE apparatus
- State of the Art
  - The Triple Trap Method (TTM)
  - Limitations
- Path towards 100 p.p.t. precision
  - Magnetic shimming and shielding system
  - Cooling trap

BASE 2017: $\mu_{\bar{p}}$= -2.792 847 344 1 (42) μ_{nucl}

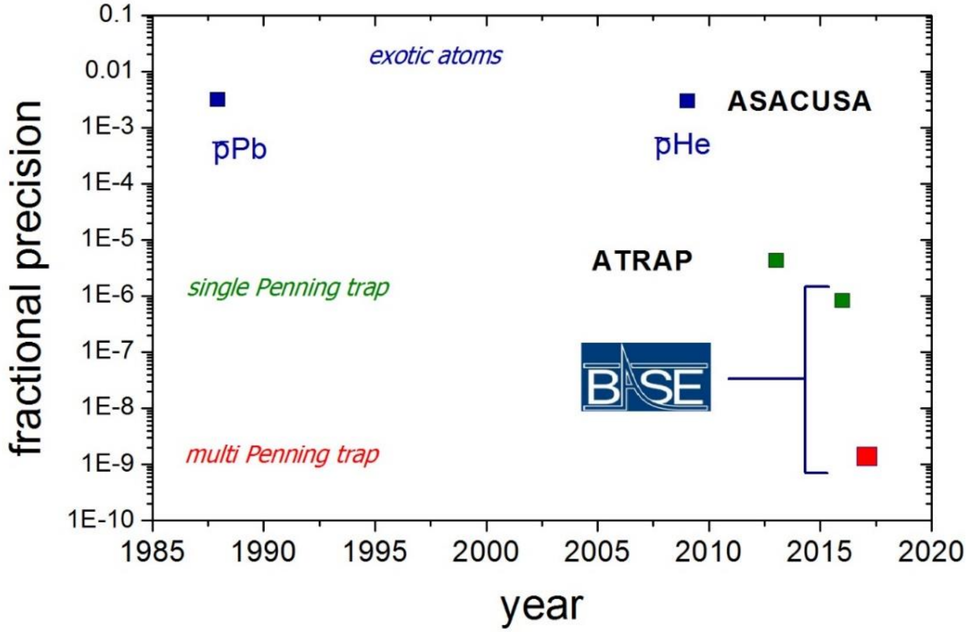

Motivation

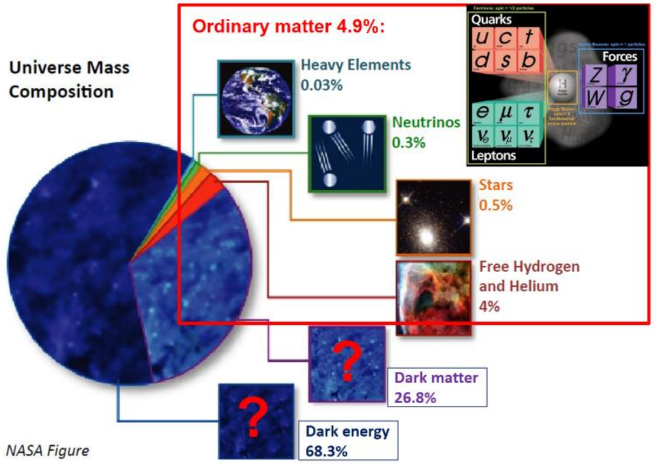

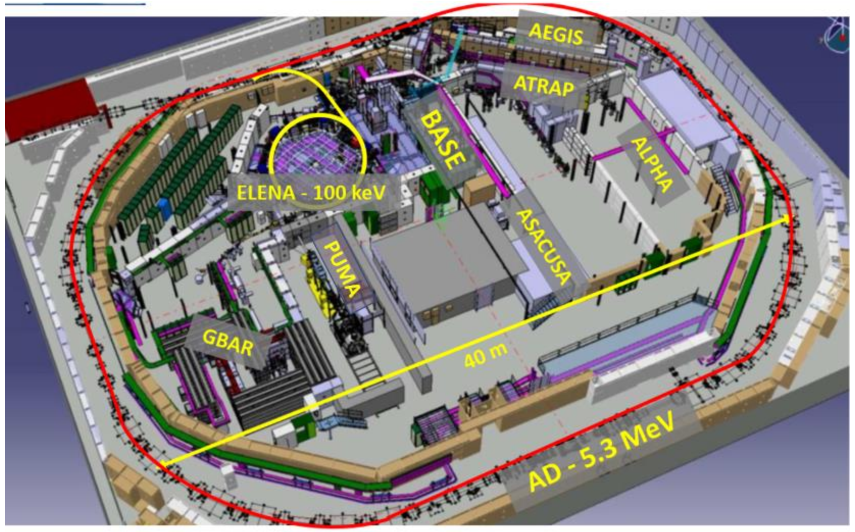

Combining Λ-CDM and Standard Model leads to 9 orders of magnitude discrepancy between prediction and observation

	Naive Expectation	Observation
Baryon/Photon Ratio	10^{-18}	0.6×10^{-9}
Baryon/Antibaryon Ratio	1	10 000

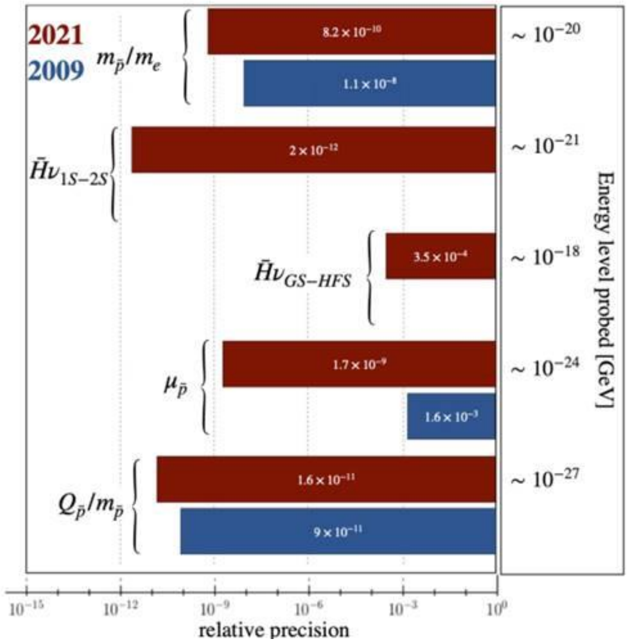

The BASE experiment

Test CPT invariance by comparing the fundamental properties of protons and antiprotons in Penning traps:

1. Charge-to-mass ratio: $\frac{\left(\frac{q}{m}\right)_{\bar{p}}}{\left(\frac{q}{m}\right)_{p}} = -1.000000000003(16)$ [1]

2. Magnetic moment: $\mu_{\bar{p}} = -2.7928473441(42)\mu_{N}$ [2]

3. Antiproton lifetime: $\tau_{\bar{p}} > 26.7$ a [3]

4. Differential test of gravitational interaction: $\left|\alpha_{g,D} - 1\right| < 0.03$ [1]

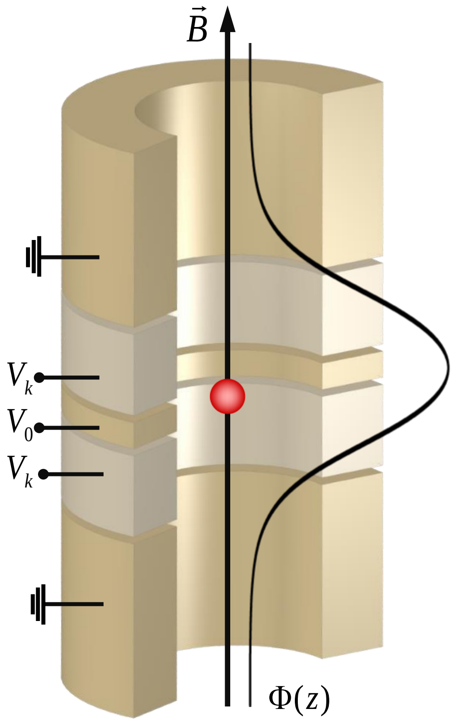

[1] S. Ulmer *et al.,* A 16-parts-per-trillion measurement of the antiproton-to-proton charge–mass ratio., *Nature* **601**, 53–57 (2022).
[2] C. Smorra *et al.,* A parts-per-billion measurement of the antiproton magnetic moment., *Nature* **550**, 371–374 (2017).
[3] M.J. Borchert, *Challenging the Standard Model by high precision comparisons of the fundamental properties of antiprotons and protons, 2021.*

The Penning trap

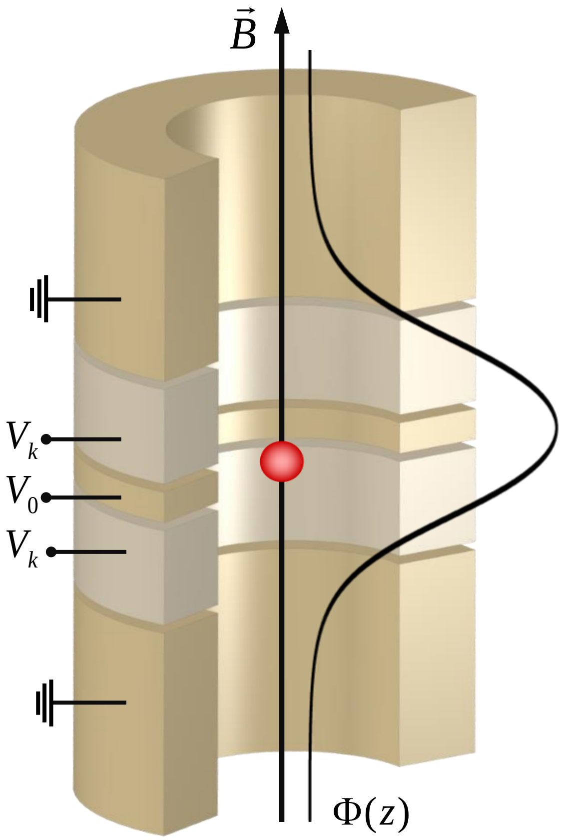

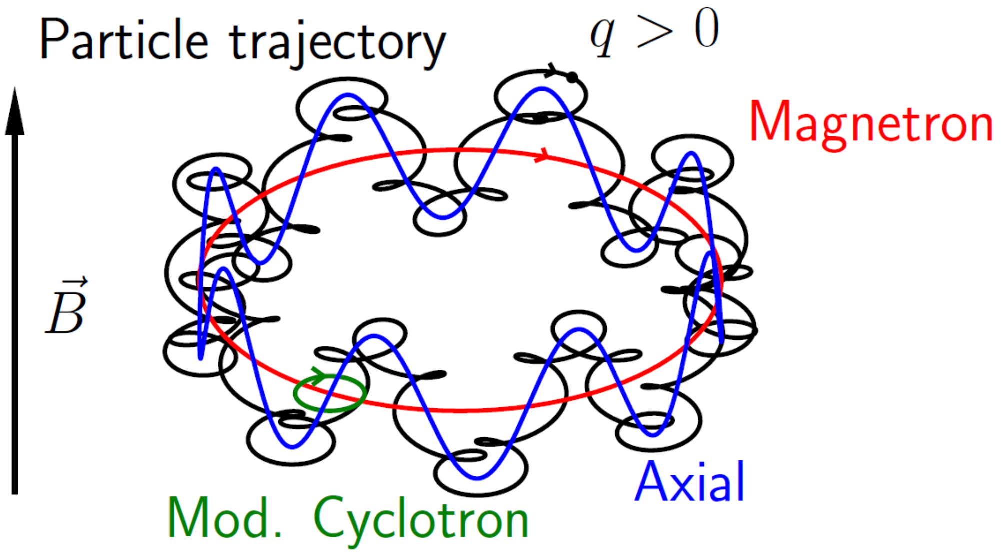

$\nu_+ \approx$ 29 MHz

$\nu_z \approx$ 650 kHz

$\nu_- \approx$ 6 kHz

$$\nu_c^2 = \nu_+^2 + \nu_z^2 + \nu_-^2$$

Measurement of the cyclotron frequency

Measure axial frequency and mod. cyclotron sidebands

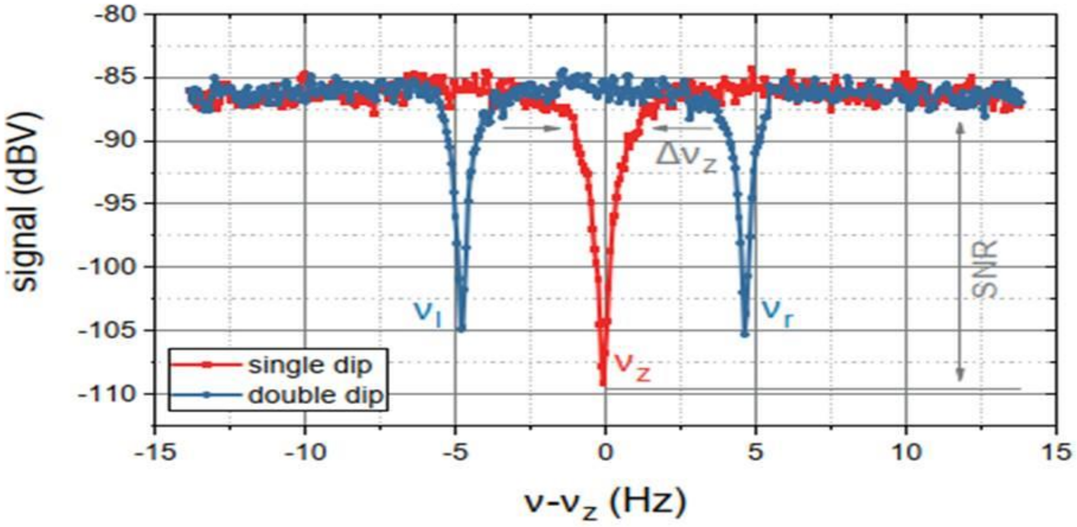

Use invariance theorem to determine free cyclotron frequency

$$\nu_c^2 = \nu_+^2 + \nu_z^2 + \nu_-^2$$

$$\nu_+ = \nu_{rf} + \nu_l + \nu_r - \nu_z$$

Note that ν_+ coupling heats the cyclotron mode

Measurement of the p-$\bar{\text{p}}$ charge-to-mass ratio

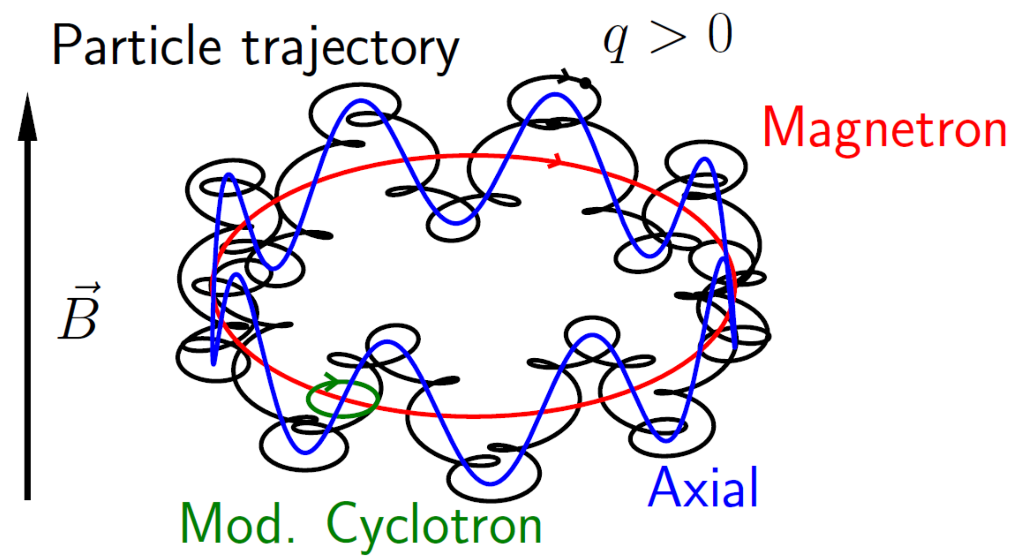

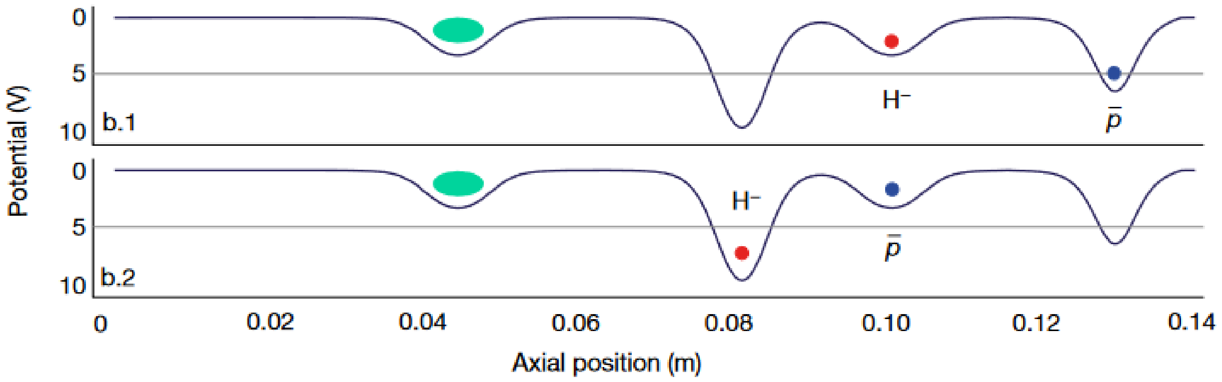

$$\nu_c^2 = \nu_+^2 + \nu_z^2 + \nu_-^2$$

$$\omega_c = \frac{q}{m} B_z$$

$$\frac{\left(\frac{q}{m}\right)_{\bar{p}}}{\left(\frac{q}{m}\right)_{\mathrm{H}^-}} = 1.001089218781$$

Measurement of the p-p̄ charge-to-mass ratio

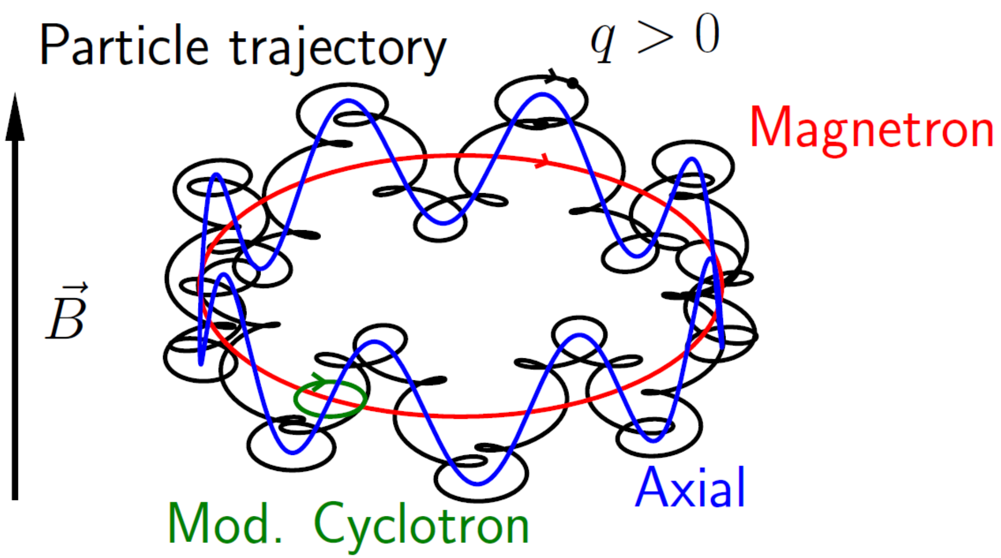

$$\nu_c^2 = \nu_+^2 + \nu_z^2 + \nu_-^2$$

$$m_{\mathrm{H}^-} = m_{\mathrm{p}}\left(1 + 2\frac{m_{\mathrm{e}}}{m_{\mathrm{p}}} - \frac{E_{\mathrm{b}}}{m_{\mathrm{p}}c^2} - \frac{E_{\mathrm{a}}}{m_{\mathrm{p}}c^2} + \frac{\alpha_{\mathrm{pol,H}^-} B_0^2}{m_{\mathrm{p}}c^2}\right)$$

Effect	Magnitude	
$m_e/m_p c^2$	0.001 089 234 042 95 (5)	MPIK/ HHU-D
$-E_b/m_p c^2$	0.000 000 014 493 061 …	MPQ
$-E_a/m_p c^2$	0.000 000 000 803 81 (2)	Lykke
$\frac{\alpha_{\mathrm{pol,H}^-} B_0^2}{m_{\mathrm{p}}c^2}$	0.000 000 000 007 685 (18)	

$$\frac{\left(\frac{q}{m}\right)_{\bar{p}}}{\left(\frac{q}{m}\right)_p} = -1.000000000003(16)$$

Measurement of the p-$\bar{p}$ charge-to-mass ratio

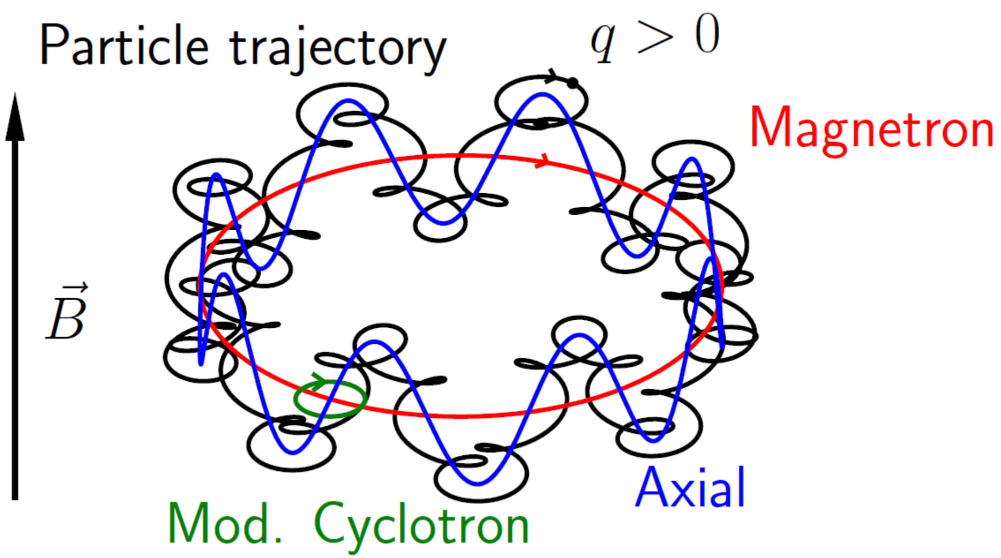

$$\nu_c^2 = \nu_+^2 + \nu_z^2 + \nu_-^2$$

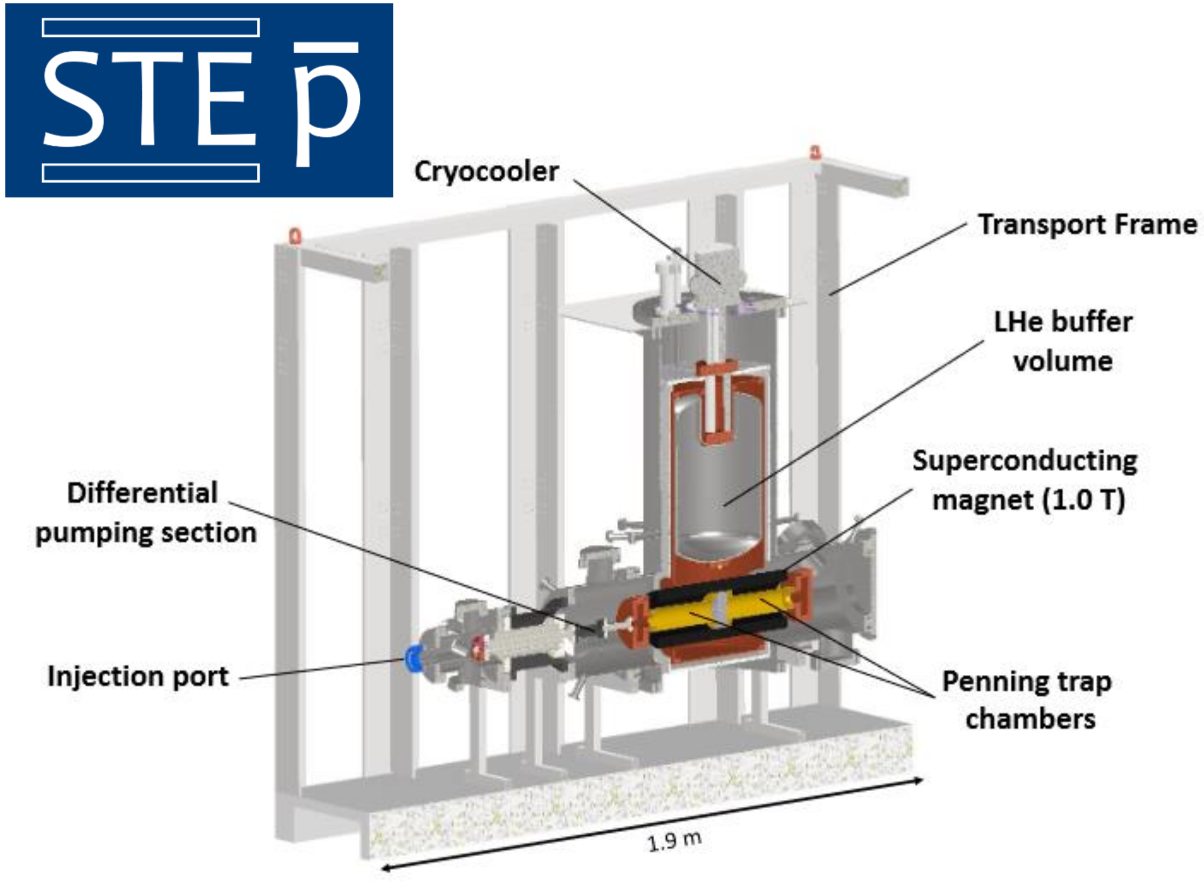

Preparing for beam taking in 2022

Measurement of the antiproton *g*-factor

$$\overrightarrow{\mu_S} = g\,\frac{q}{2m}\vec{S}$$

Measurement of the antiproton *g*-factor

$$\Delta E = g \frac{q\hbar}{2m} B_z$$

Measurement of the antiproton *g*-factor

$$\omega_L = g \frac{q}{2m} B_z$$

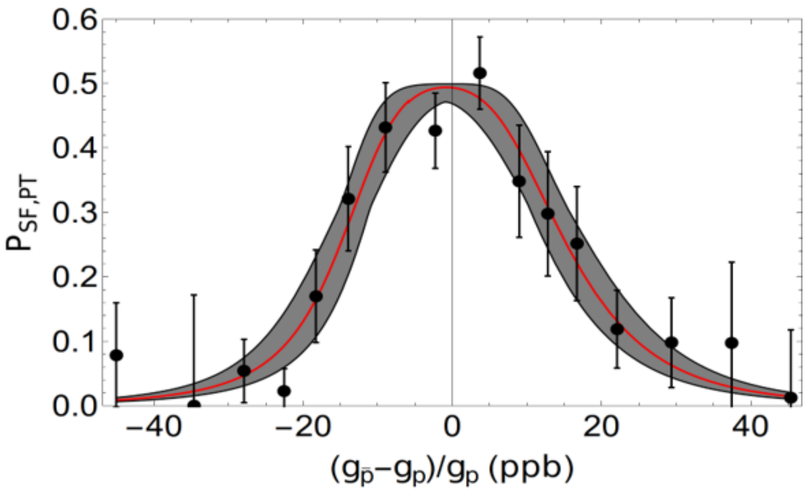

Measurement of the antiproton *g*-factor

$$\omega_L = g \frac{q}{2m} B_z$$

$$\omega_c = \frac{q}{m} B_z$$

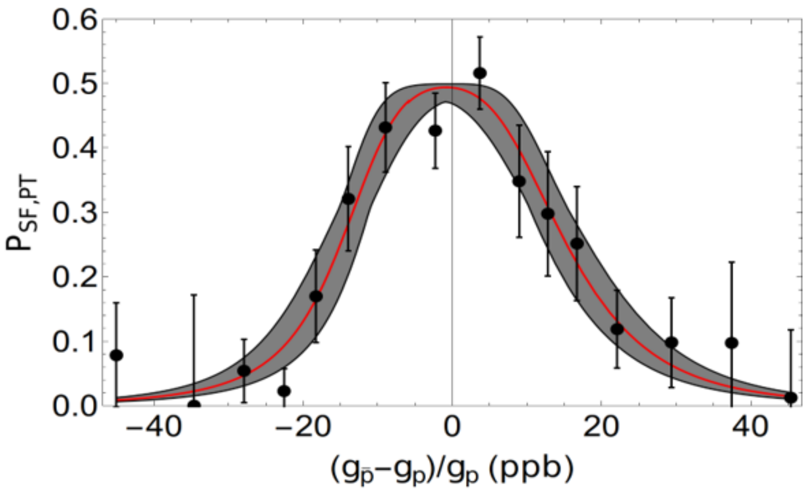

Measurement of the antiproton *g*-factor

$$\omega_L = g\frac{q}{2m}B_z$$

$$\omega_c = \frac{q}{m}B_z$$

$$g = 2\frac{\omega_L}{\omega_c}$$

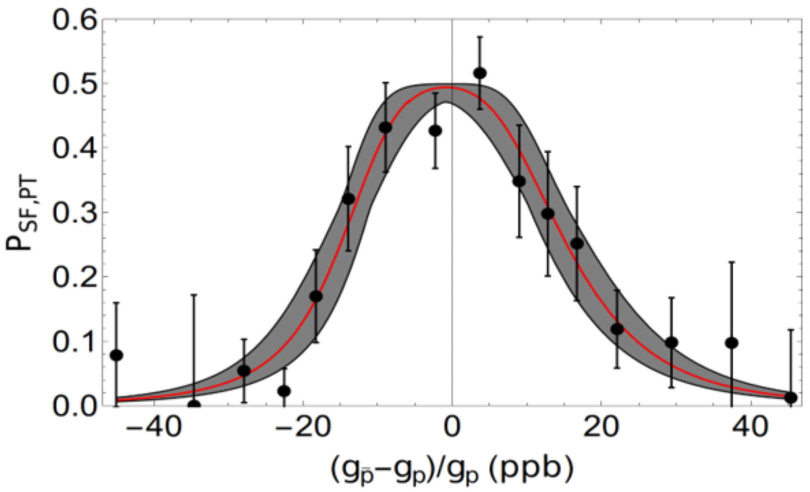

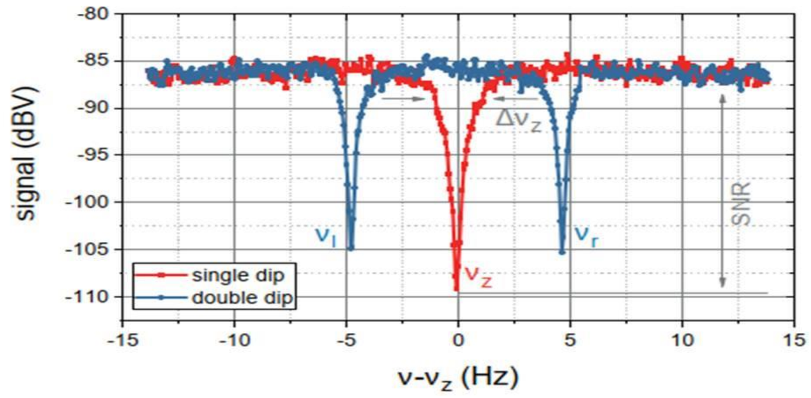

The BASE multi-trap stack

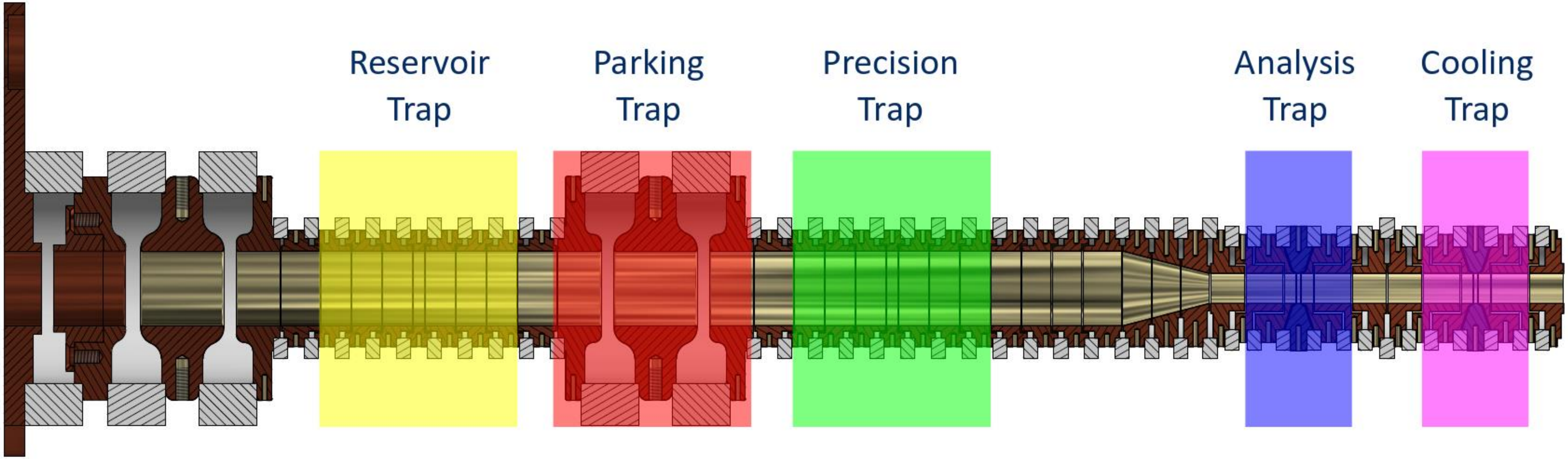

The BASE apparatus

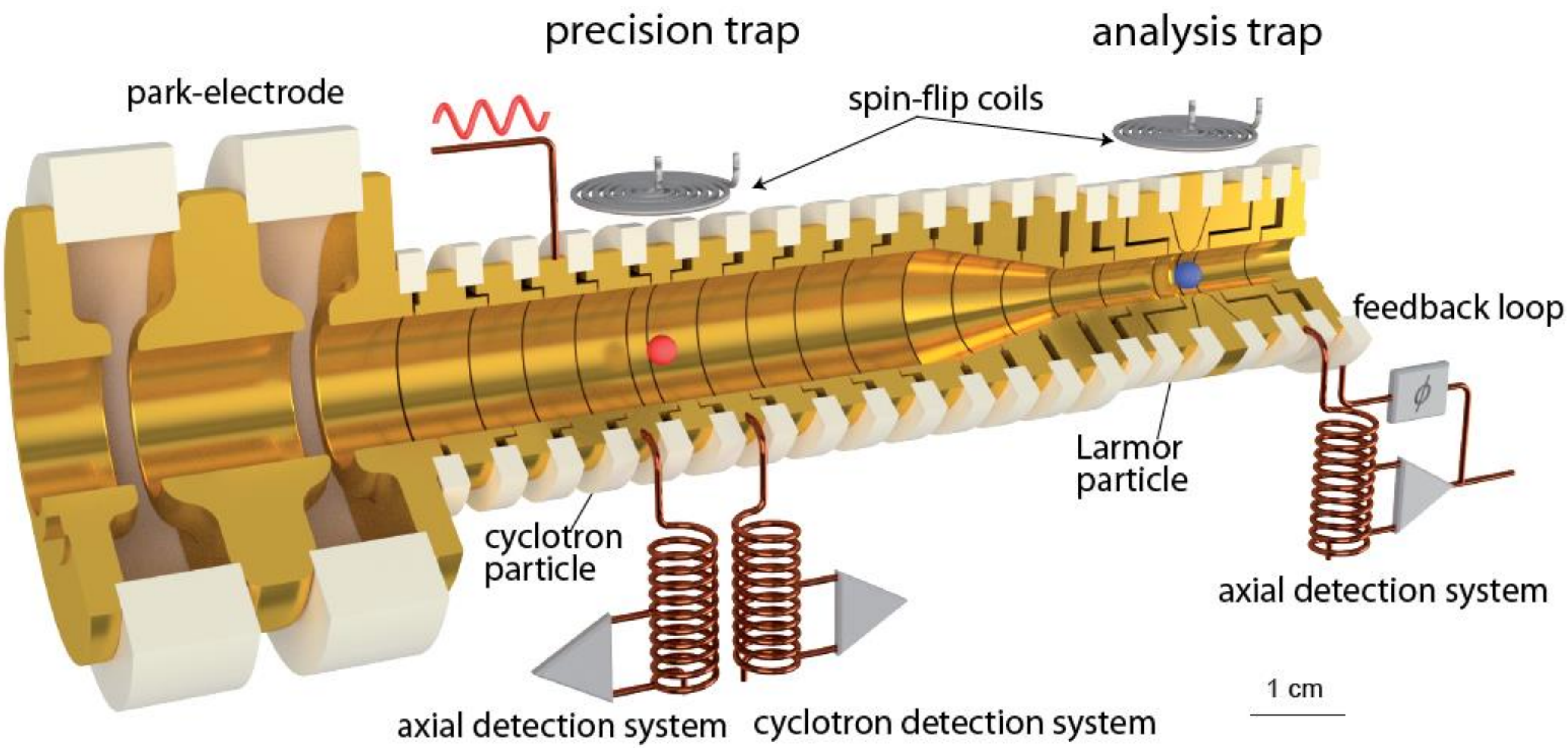

Axial detection system

Resonator

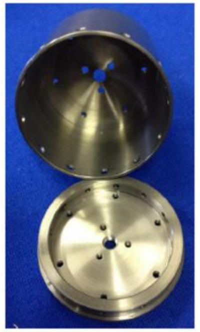

Toroidal coil

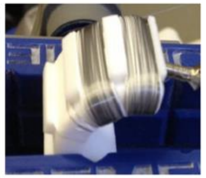

N = 950 – 1200
Q = 200k – 500k
L = 2-3 mH
Rp > 1 GΩ

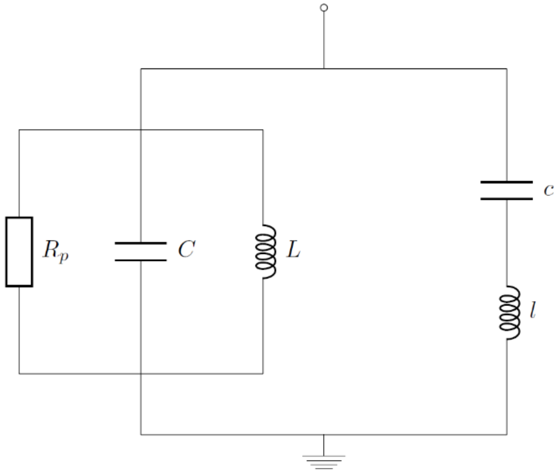

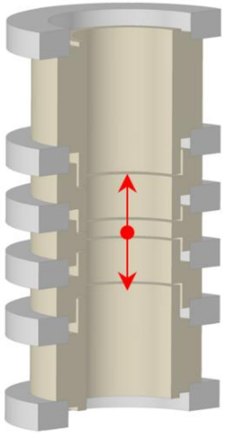

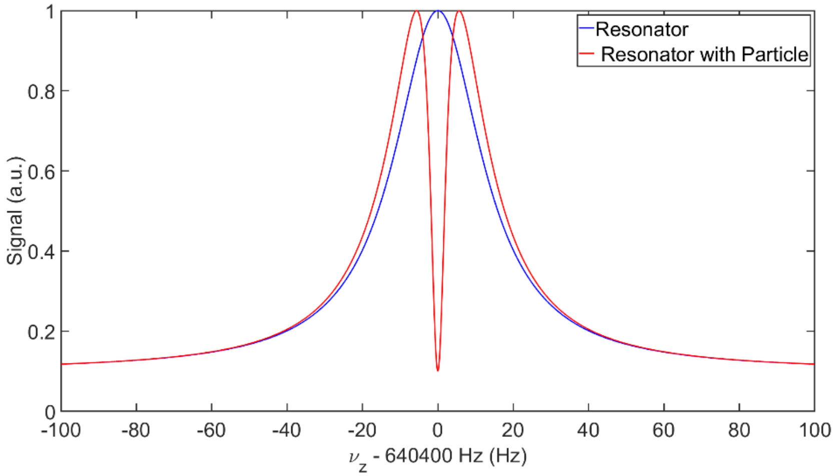

$$\mathrm{Re}(Z) = \frac{R_P}{1 + \left[\frac{\frac{Q}{\omega_0}(\omega^2 - \omega_P^2)(\omega_0^2 - \omega^2) + \gamma\omega}{\omega(\omega^2 - \omega_P^2)}\right]}$$

Spin state detection

2. Determination of ω_L

Couple spinstate to axial frequency by superimposing a magnetic bottle ($B_2 \approx 300\,000$ T m^{-2})

$$\Delta\omega_z = \frac{\hbar\,\omega_+}{m\,\omega_z}\frac{B_2}{B_0}\left(\left(n_+ + \frac{1}{2}\right) + \frac{\omega_-}{\omega_+}\left(n_- + \frac{1}{2}\right) + m_s\frac{g}{2}\right)$$

$$\Delta\nu_+ \approx 62\,mHz$$
$$\Delta\nu_- \approx 0.04\,mHz$$
$$\Delta\nu_S \approx 172\,mHz$$

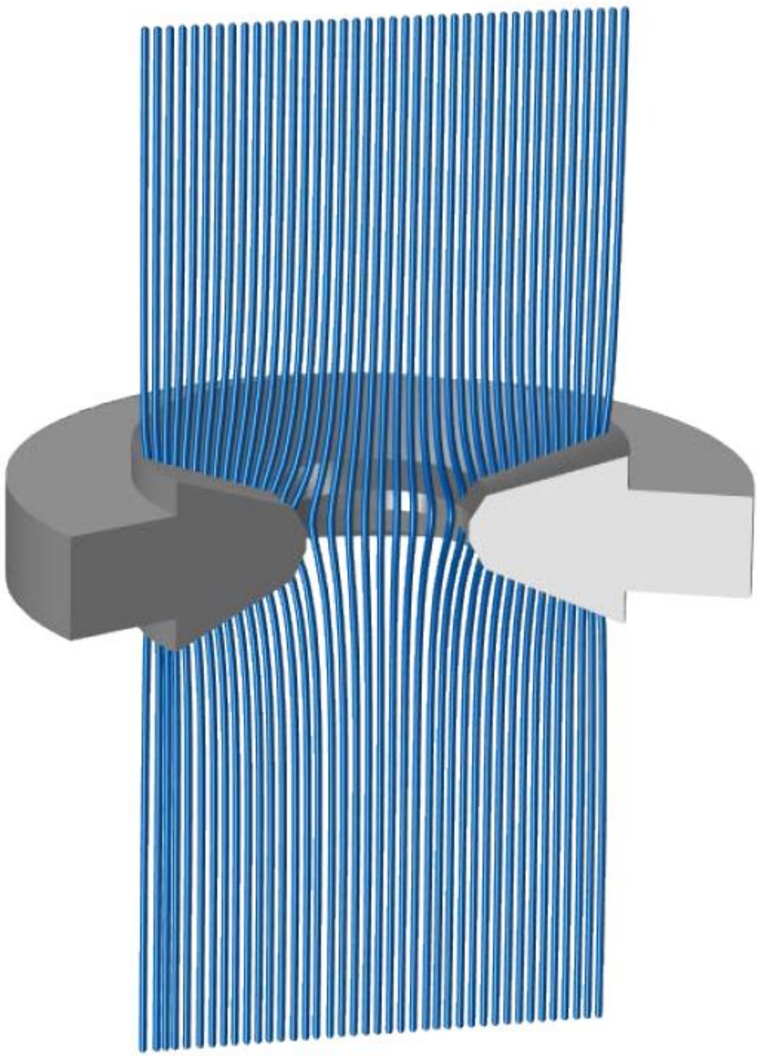

Spin state detection

Couple spinstate to axial frequency by superimposing a magnetic bottle ($B_2 \approx 300\,000$ T m^{-2})

$$\Delta\omega_z = \frac{\hbar\,\omega_+}{m\,\omega_z}\frac{B_2}{B_0}\left(\left(n_+ + \frac{1}{2}\right) + \frac{\omega_-}{\omega_+}\left(n_- + \frac{1}{2}\right) + m_s\frac{g}{2}\right)$$

$$\Delta\nu_+ \approx 62\,mHz$$
$$\Delta\nu_- \approx 0.04\,mHz$$
$$\Delta\nu_S \approx 172\,mHz$$

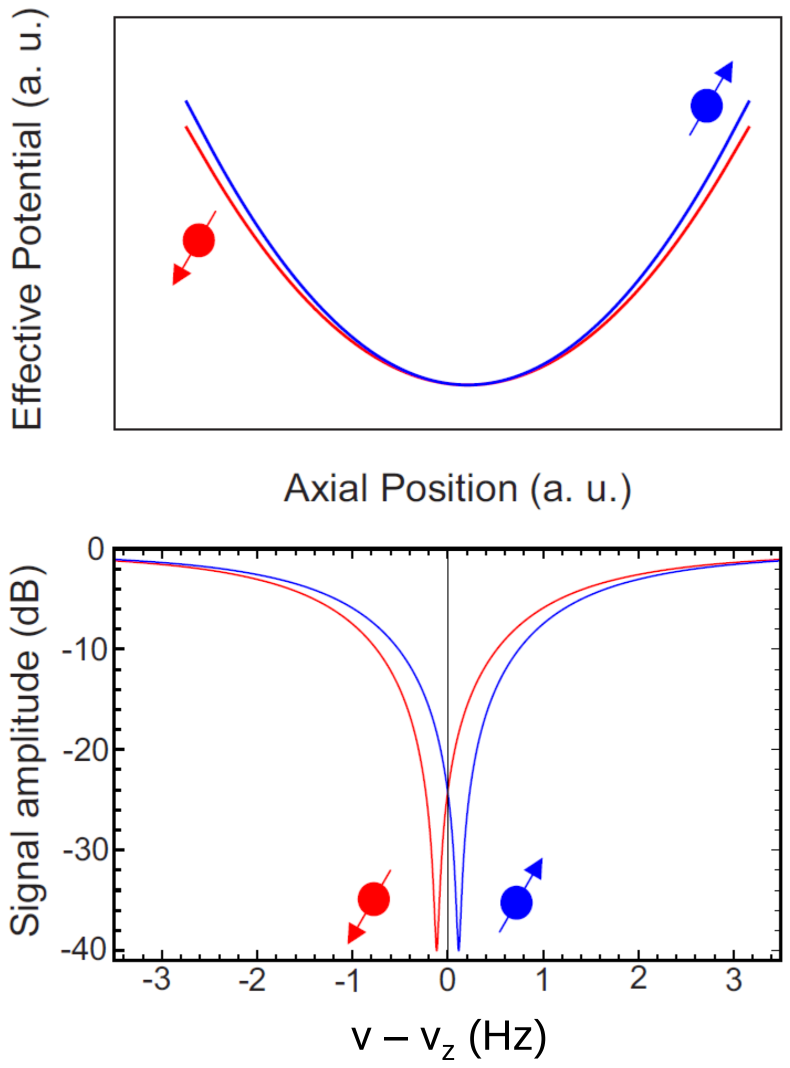

SMORRA, Christian, et al. Base–the baryon antibaryon symmetry experiment. *The European Physical Journal Special Topics*, 2015, 224. Jg., Nr. 16, S. 3055-3108.

Spin state detection

Couple spinstate to axial frequency by superimposing a magnetic bottle ($B_2 \approx 300\,000$ T m^{-2})

$$\Delta\omega_z = \frac{\hbar\,\omega_+}{m\,\omega_z}\frac{B_2}{B_0}\left(\left(n_+ + \frac{1}{2}\right) + \frac{\omega_-}{\omega_+}\left(n_- + \frac{1}{2}\right) + m_s\frac{g}{2}\right)$$

Probe spinflip probability as function of drive frequency ω_{RF}

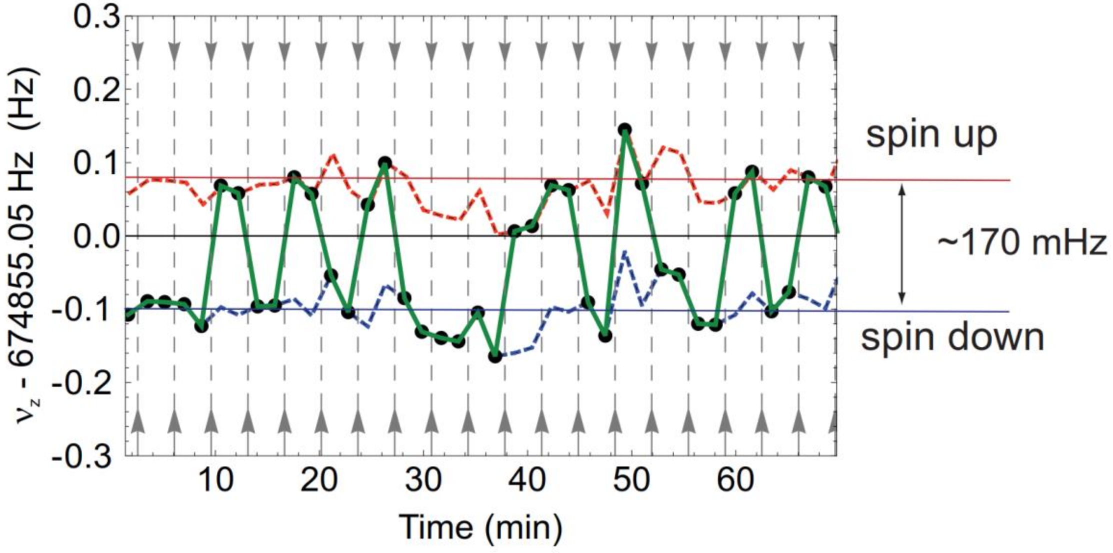

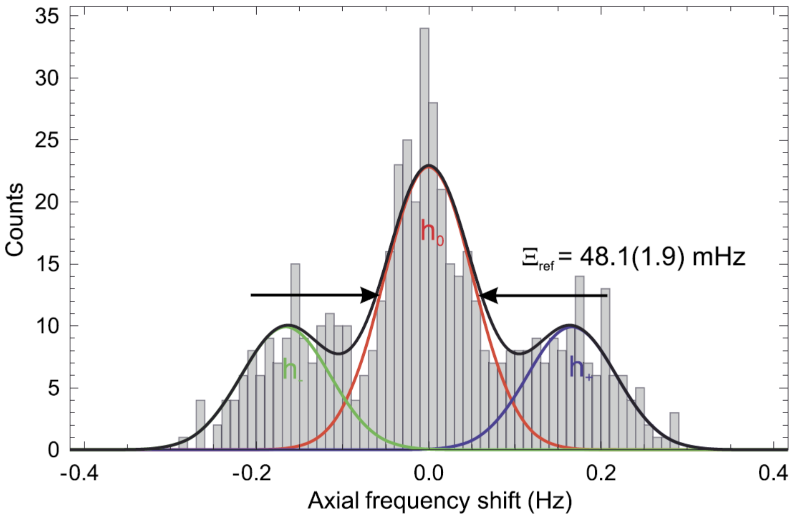

SMORRA, Christian, et al. Observation of individual spin quantum transitions of a single antiproton. *Physics Letters B*, 2017, 769. Jg., S. 1-6.

The Triple Trap Method

Cyclotron heating rate increases with cyclotron temperature

$$\zeta_+ = n_+ \frac{q^2}{2\hbar m\,\omega_+} S_E(\omega_+)$$

Measurement requires cold particle
→ Cooling

cold particle (50mK)

hot particle (1K)

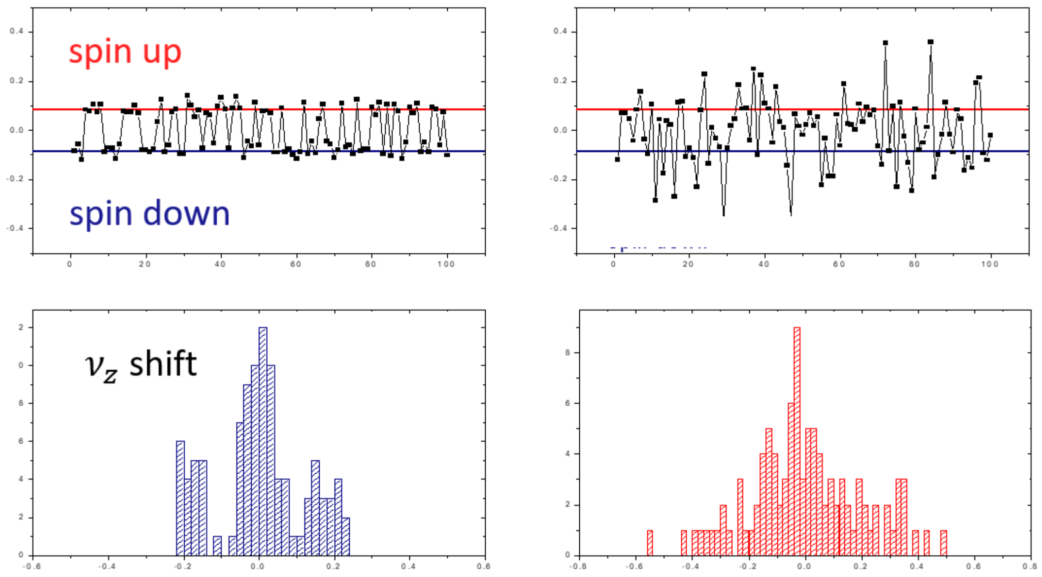

Subthermal cooling

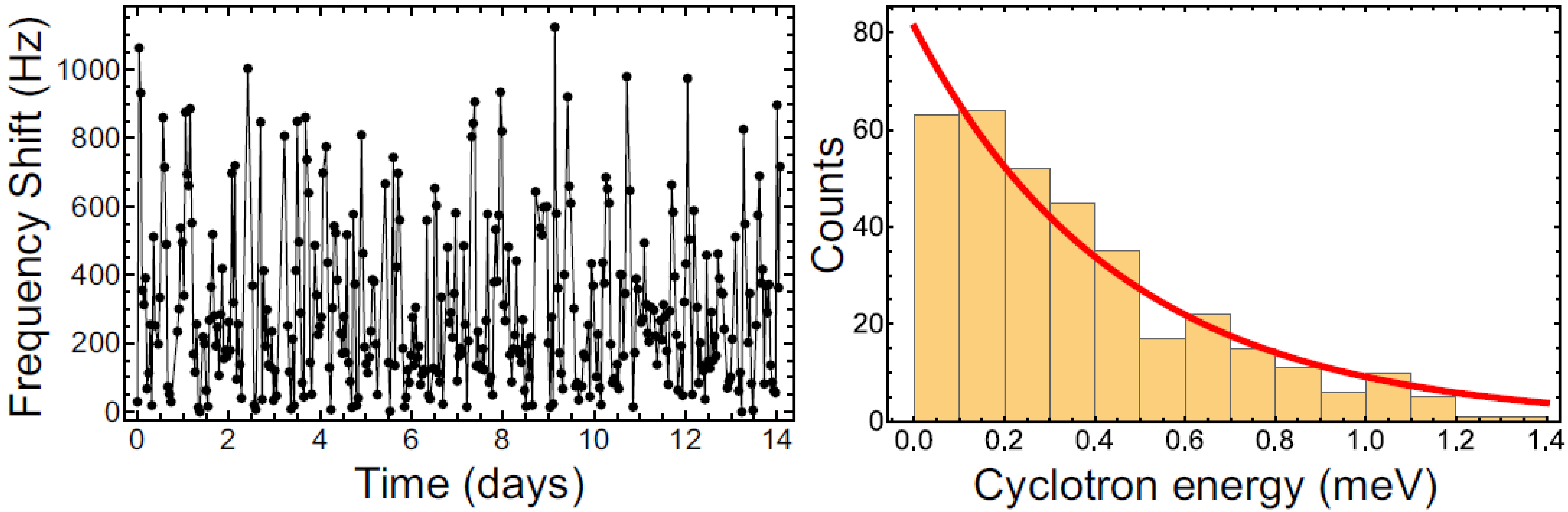

200 mK temperature acceptance → 15 h preparation time

The Triple Trap Method

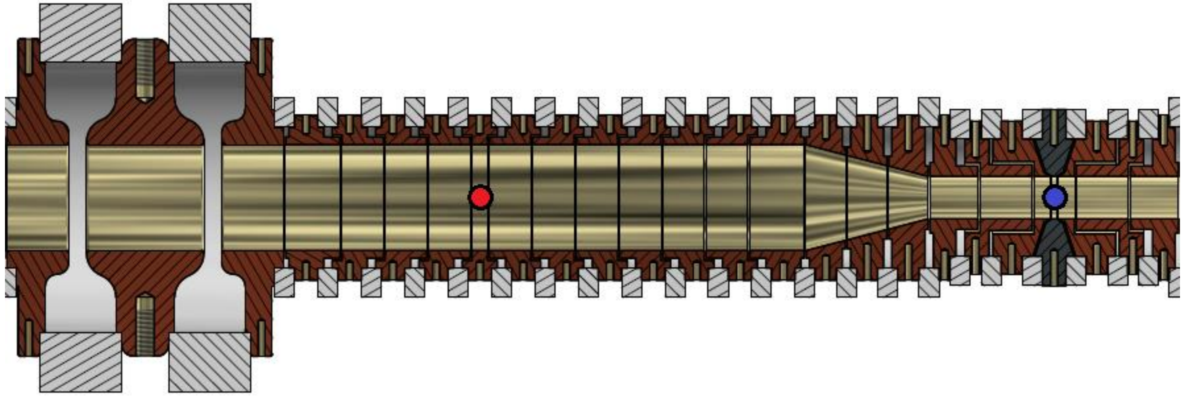

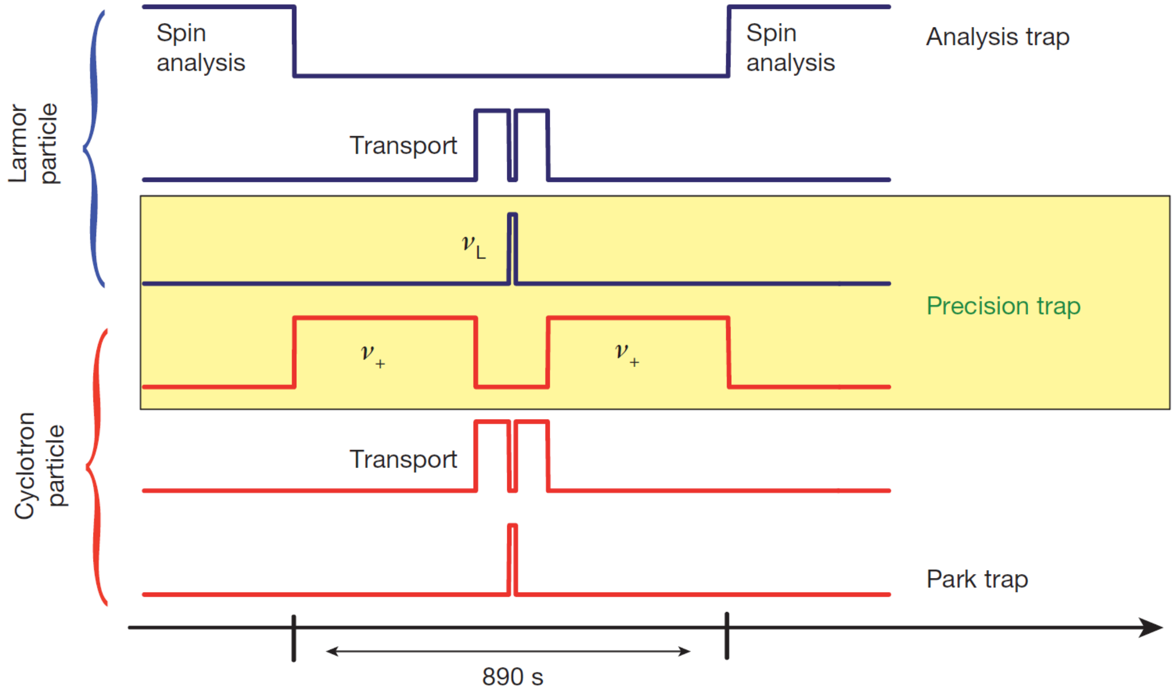

SMORRA, C., et al. A parts-per-billion measurement of the antiproton magnetic moment. *Nature*, 2017, 550. Jg., Nr. 7676, S. 371.

The Triple Trap Method

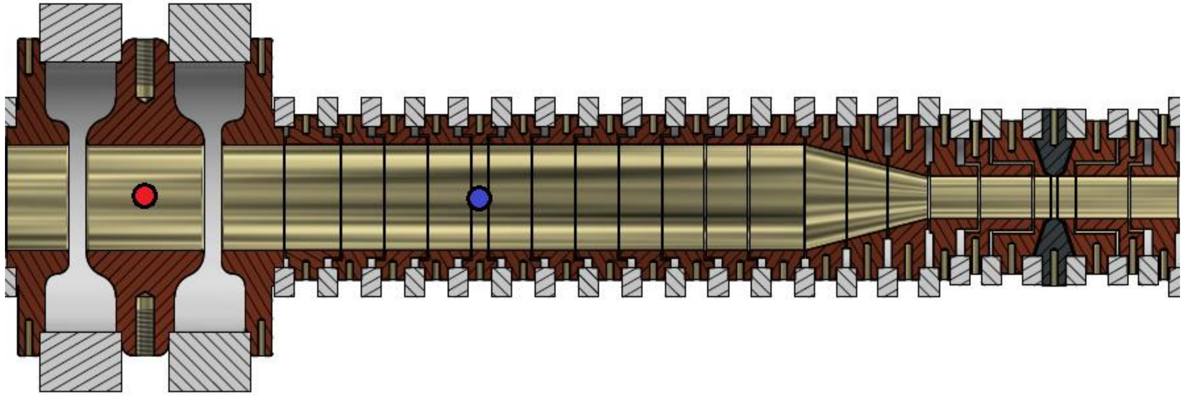

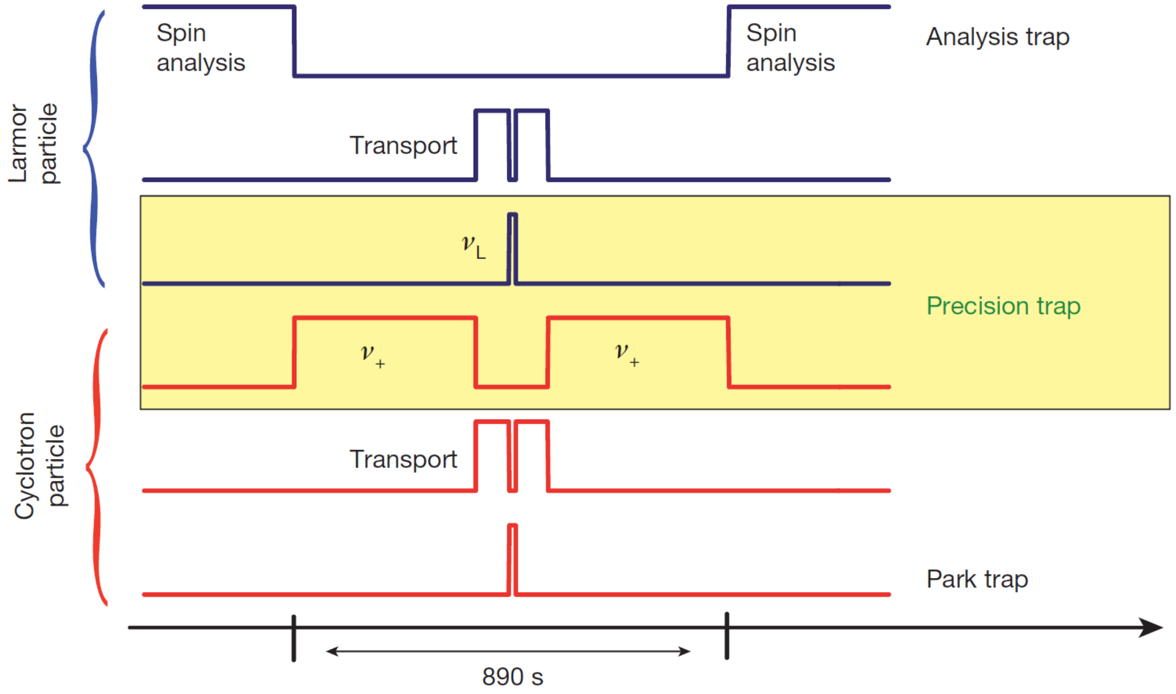

SMORRA, C., et al. A parts-per-billion measurement of the antiproton magnetic moment. *Nature*, 2017, 550. Jg., Nr. 7676, S. 371.

The Triple Trap Method

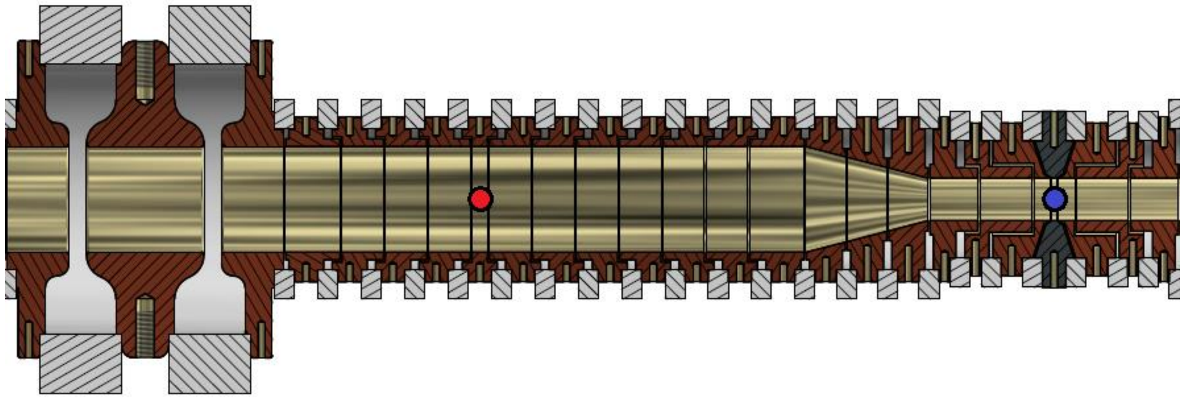

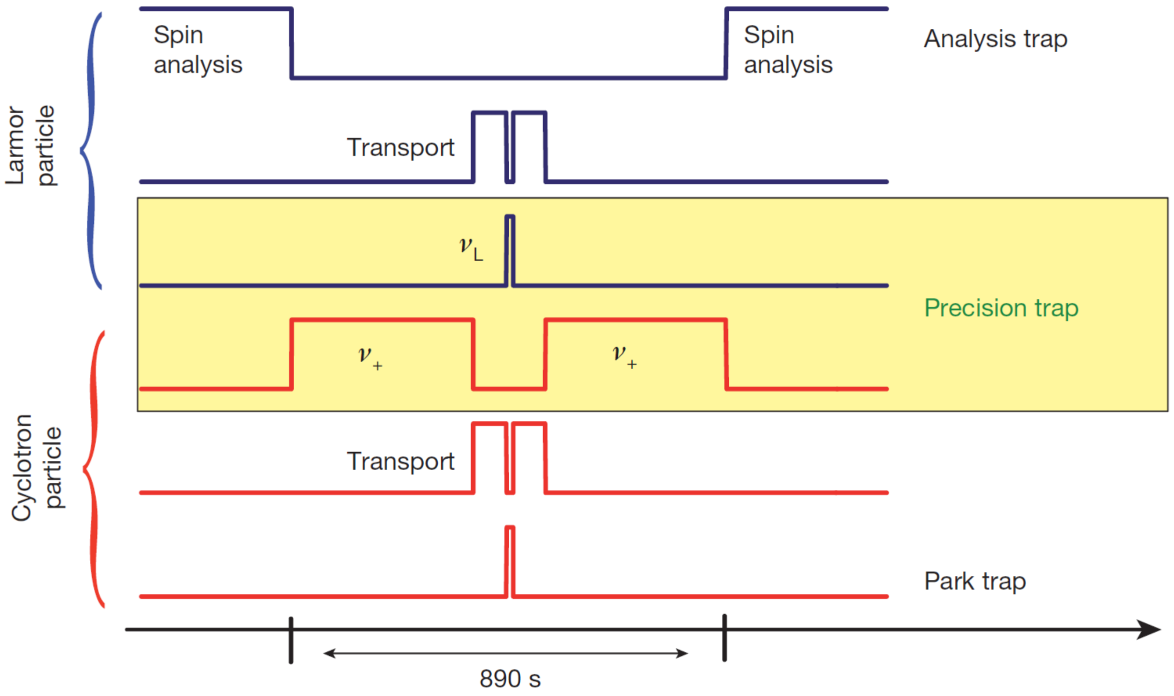

SMORRA, C., et al. A parts-per-billion measurement of the antiproton magnetic moment. *Nature*, 2017, 550. Jg., Nr. 7676, S. 371.

Limitations

Effect	Correction (p.p.b.)	Uncertainty (p.p.b.)
Image-charge shift	0.05	0.001
Relativistic shift	0.03	0.003
Magnetic gradient	0.22	0.020
Magnetic bottle	0.12	0.009
Trap potential	−0.01	0.001
Voltage drift	0.04	0.020
Contaminants	0.00	0.280
Drive temperature	0.00	0.970
Spin-state analysis	0.00	0.130
Total systematic shift	0.44	1.020

Limitations

1. Contaminants
   → Compare charge-to-mass ratio for both particles [1]
   → Limited by statistics of comparison measurement

2. Drive temperature
   → Larmor drive could change axial temperature of Larmor particle
   → ω_L and ω_C are probed at different magnetic fields

3. Spin-state analysis
   → Spinflip detection is stochastic process with 80% - 90% fidelity
   → Uncertainty in cyclotron fluctuations

[1] S. Ulmer *et al.,* A 16-parts-per-trillion measurement of the antiproton-to-proton charge–mass ratio., *Nature* **601**, 53–57 (2022)

Magnetic inhomogeneity

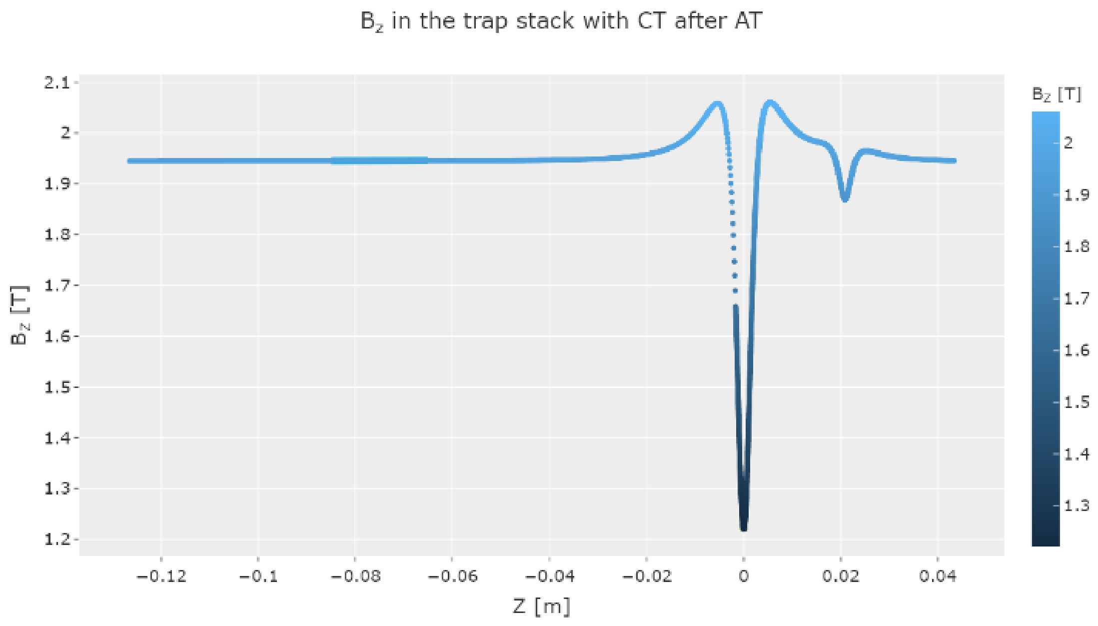

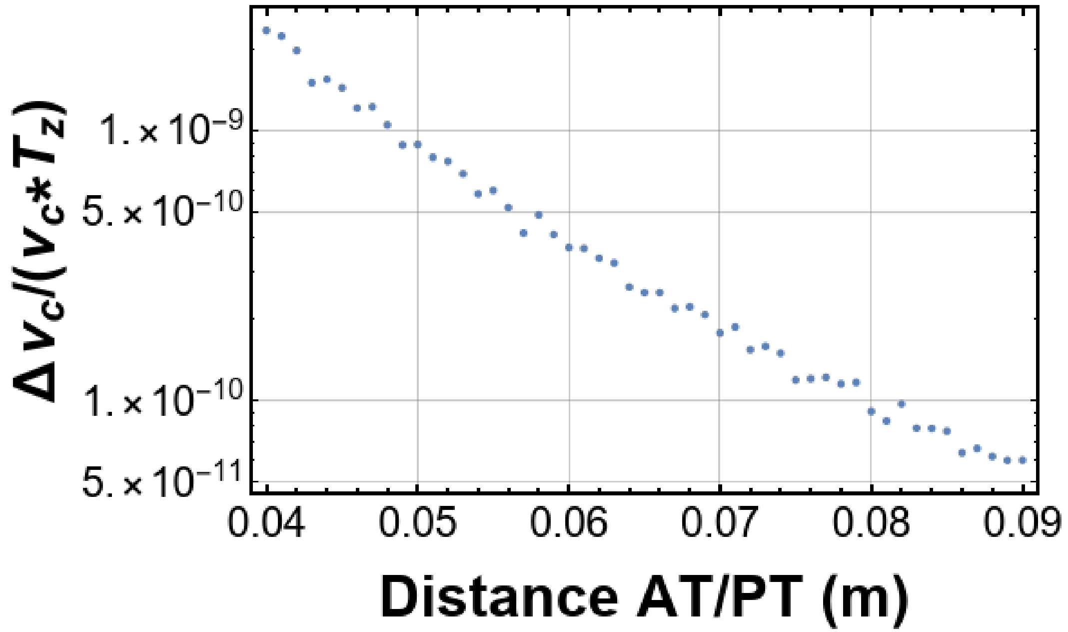

Parameter	2017	2022
B_2 [T/m^2]	2.74(22)	0.1035(2)
B_1 [T/m]	0.0712(4)	0.0252(1)

→ 970 p.p.b. systematic shift suppressed by a factor 20

Redesigned trap stack

2017:

2020:

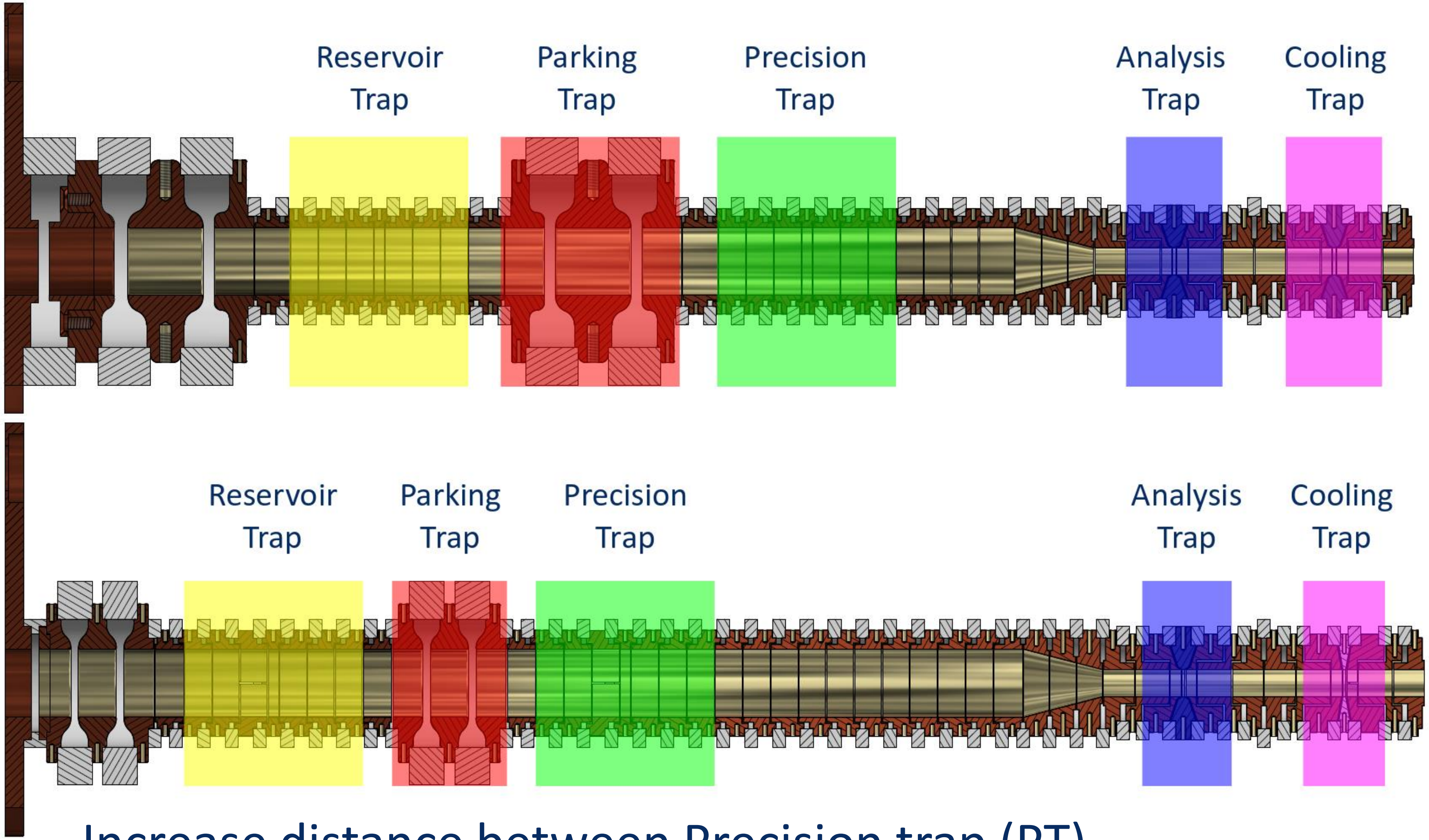

Increase distance between Precision trap (PT) and Analysis trap (AT) by 2.5 cm.

Magnetic shimming and shielding system

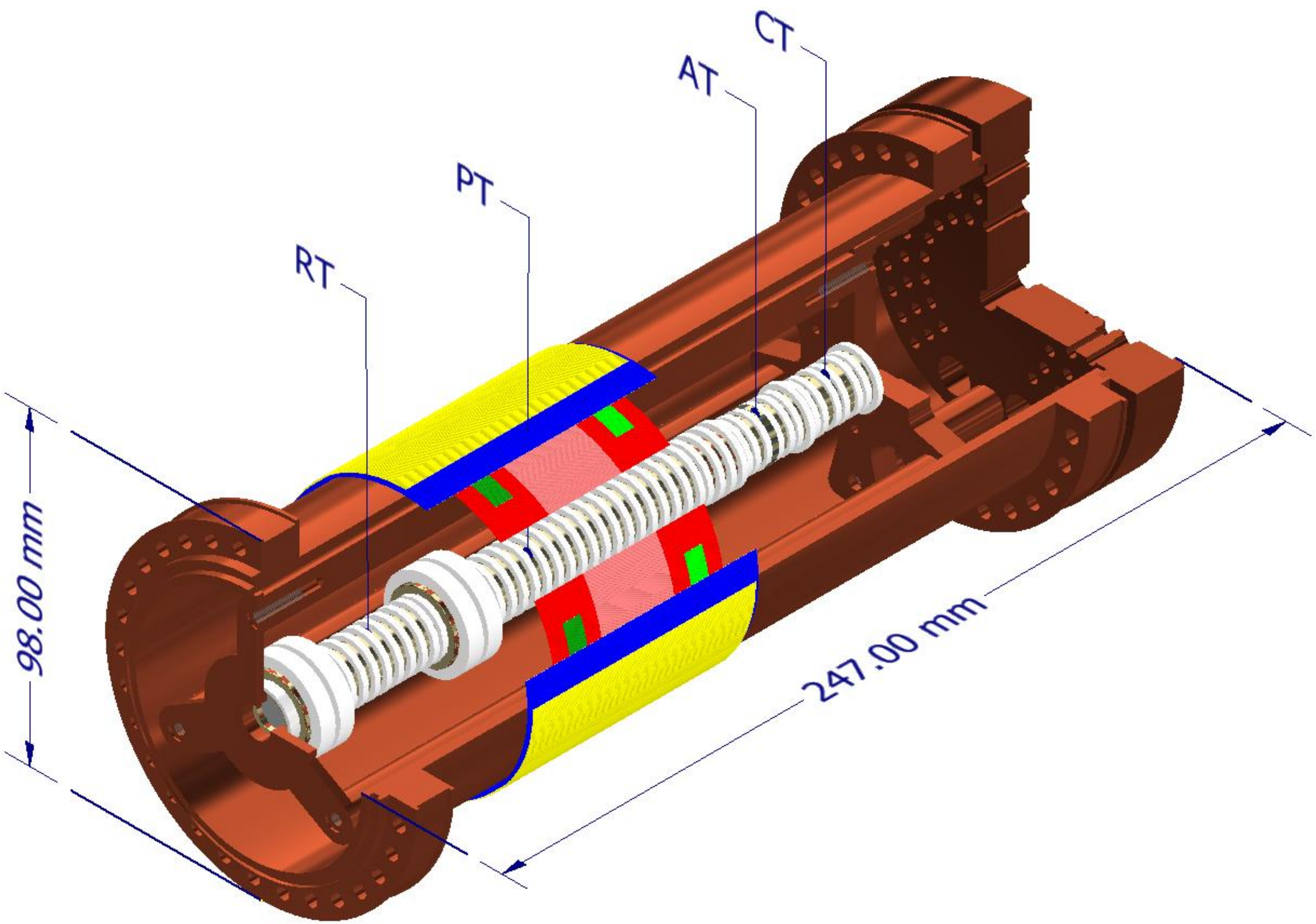

Magnetic shimming and shielding system

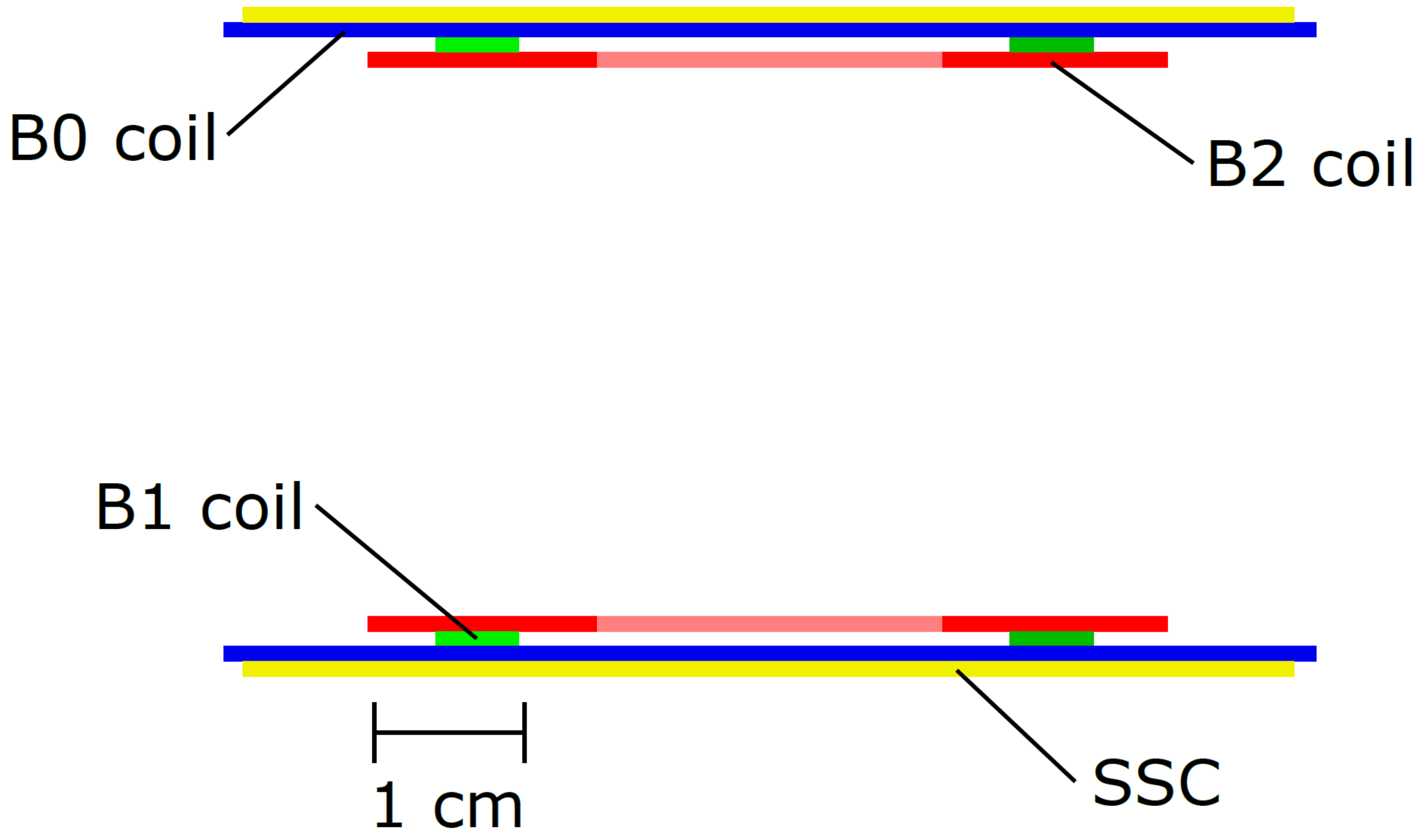

Coil system transfer functions

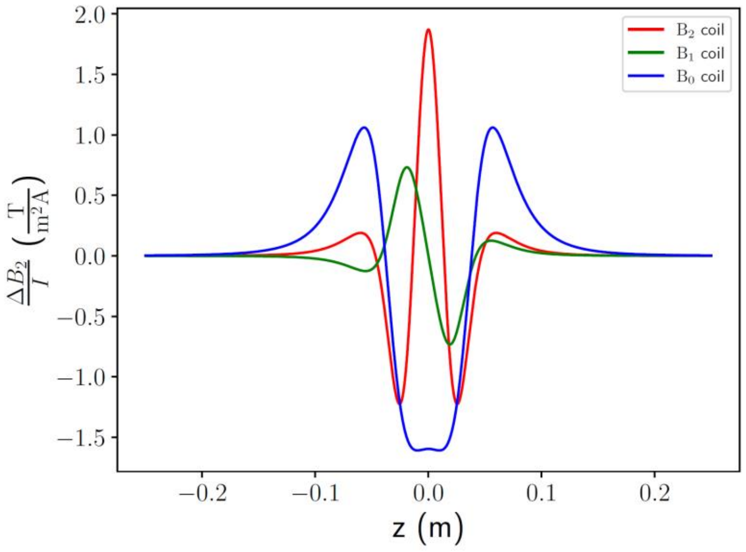

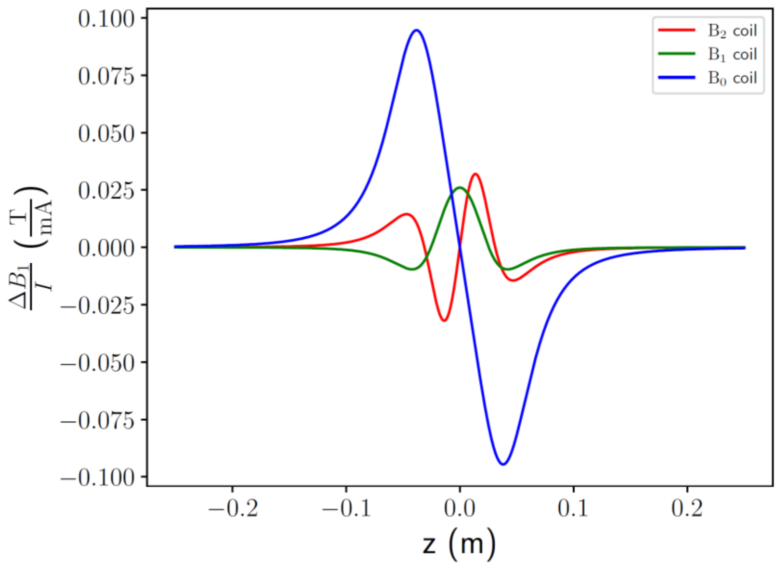

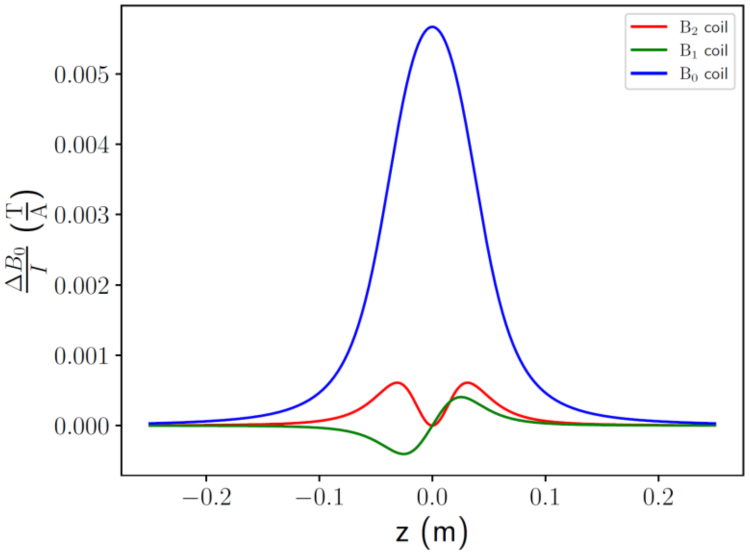

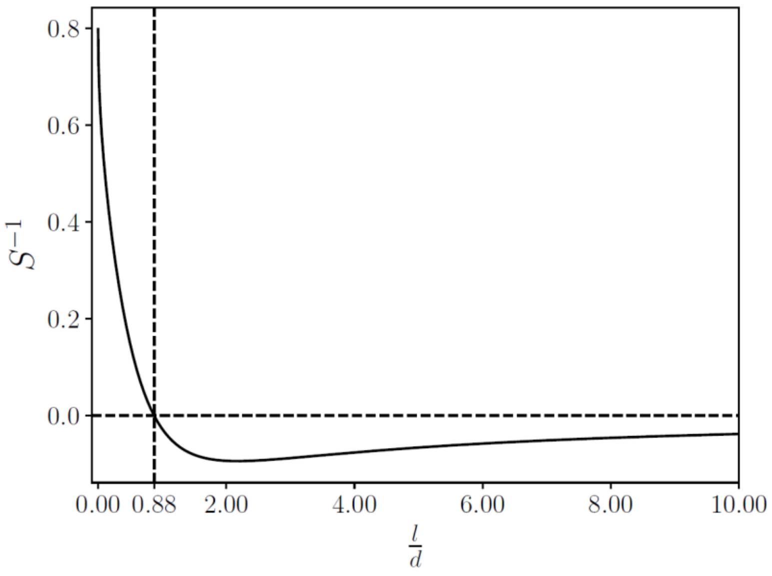

B_2 coil characterization

B2 coil transfer function

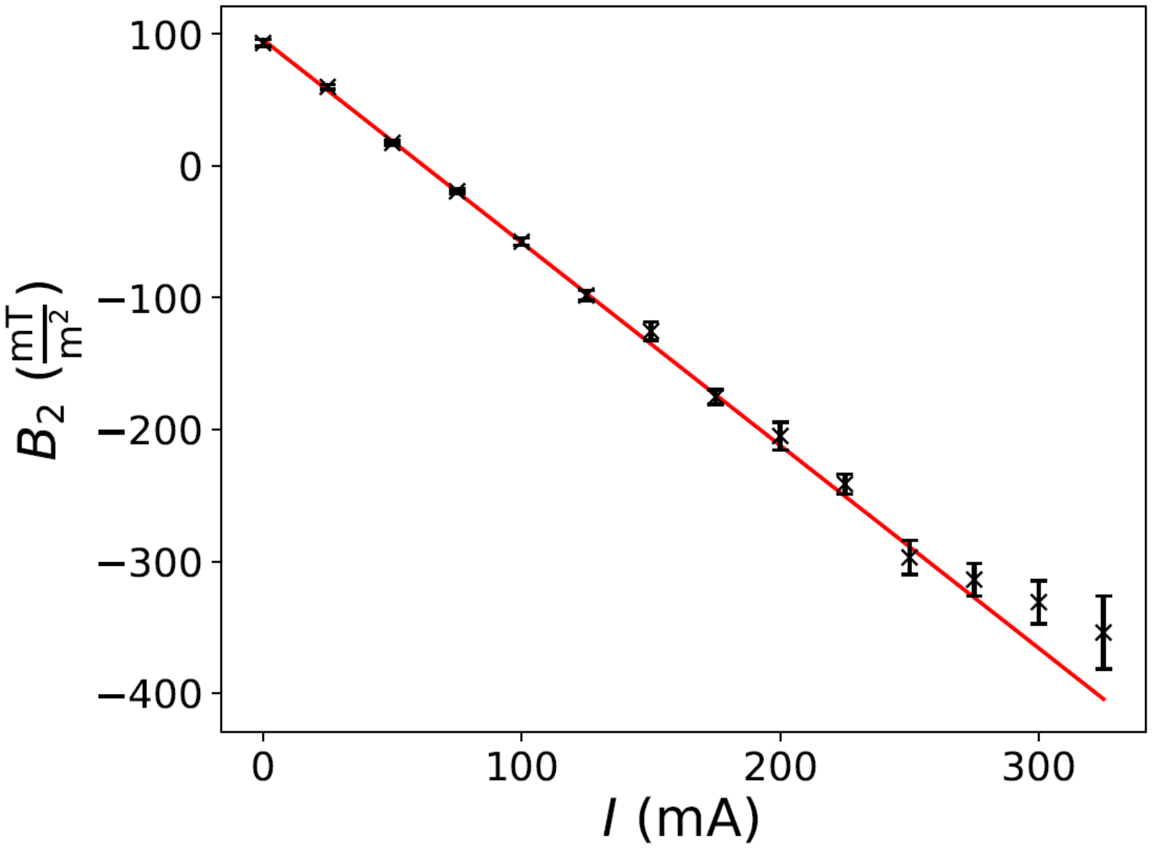

Loading reproducibility

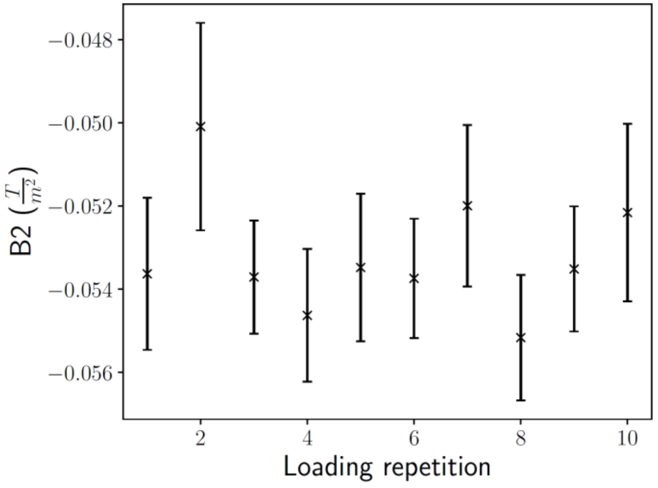

Loading stability

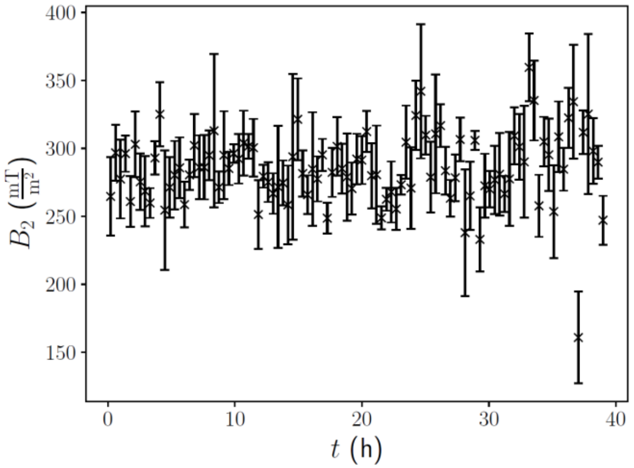

B_2 coil characterization

Compare cyclotron frequency ratio between particles of different temperature:

Ratio becomes insensitive to axial temperature as B_2 approaches 0

→ Further reduction of B_2 shifts by a factor 100

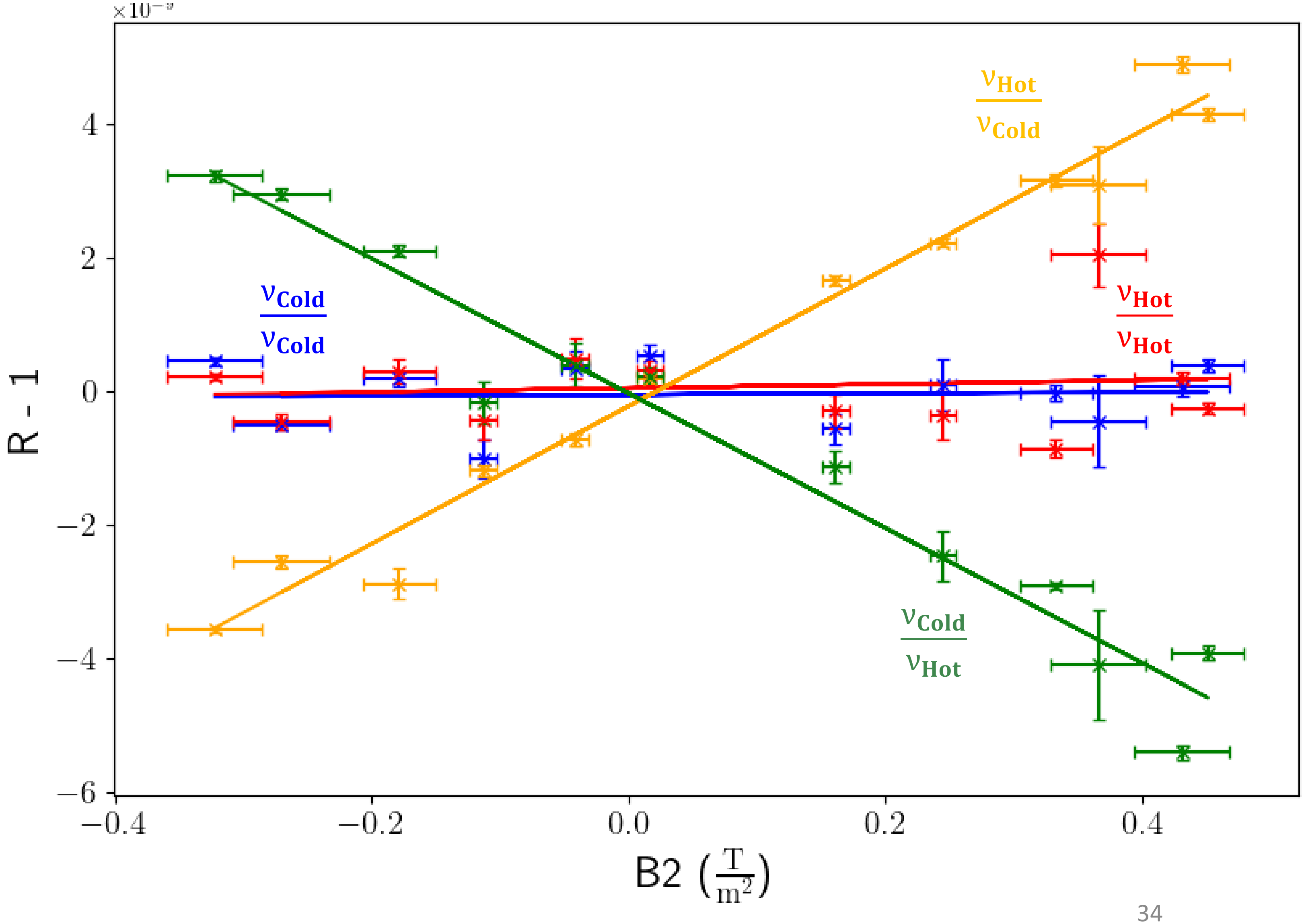

The cooling trap

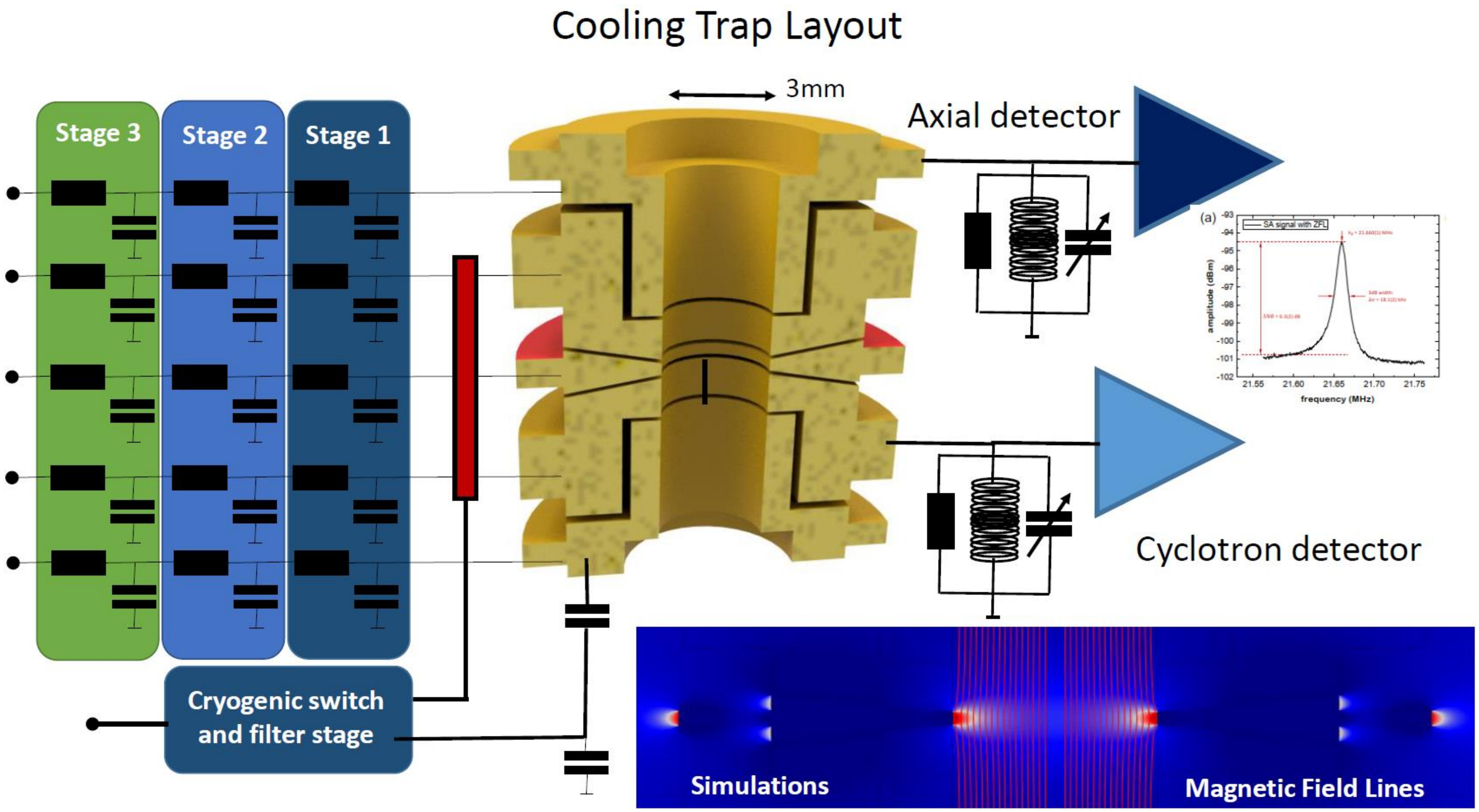

The cooling trap

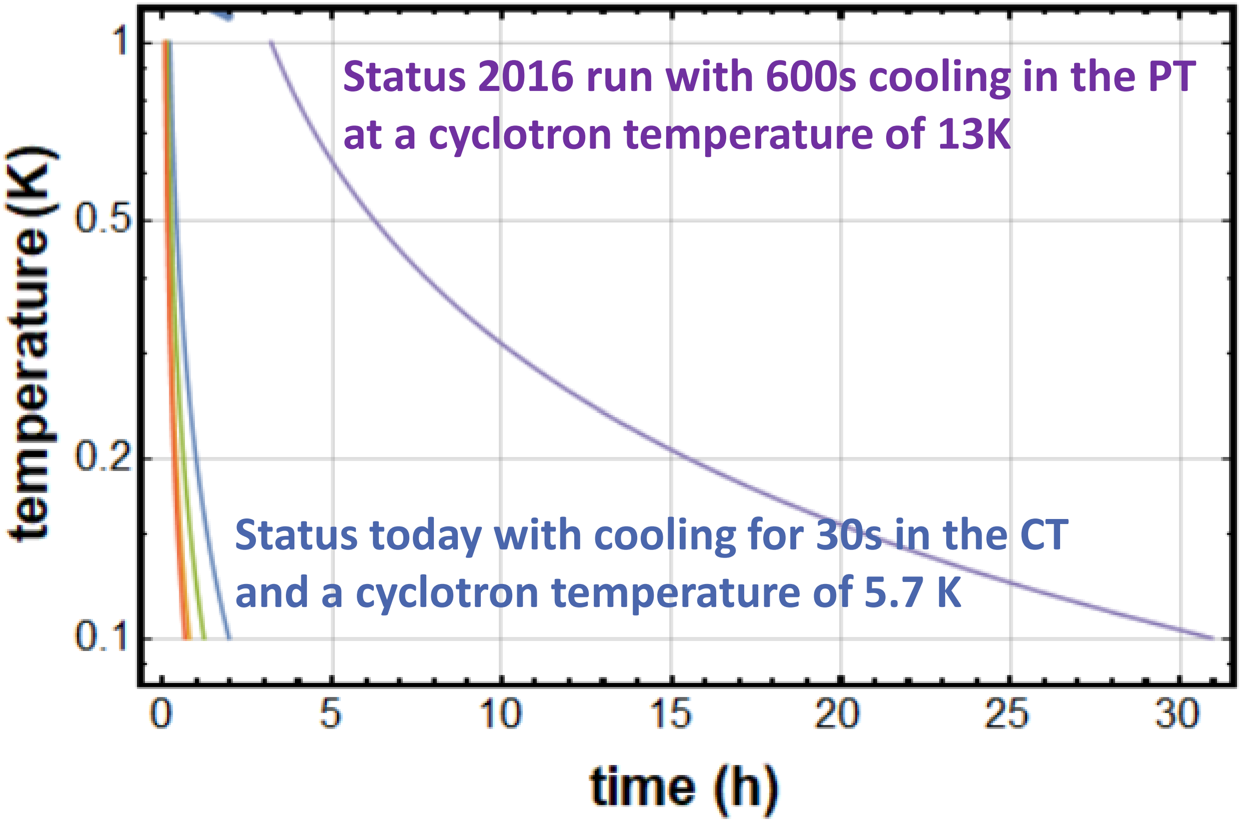

Parameter	2016 measurement (PT)	2022 measurement (CT)
Detector temperature	12.8 K	4.2 K
Detection Q	450	1250
R_p	75.000 Ω	360.000 Ω
Pickup length (D_{eff})	21.5 mm	4.2 mm
Thermalization time τ	380 s	3.2 s
Transport time	78 s	4.6 s
Readout time	120 s	10 s
200 mK preparation time	**15 h**	**8 min**

Further improvements

- Implementation of phase-sensitive detection methods [1]
- Modified cooling schemes (sympathetic laser cooling) [2]
- Stabilization of environmental parameters
- Development of a transportable trap (BASE-STEP) [3]

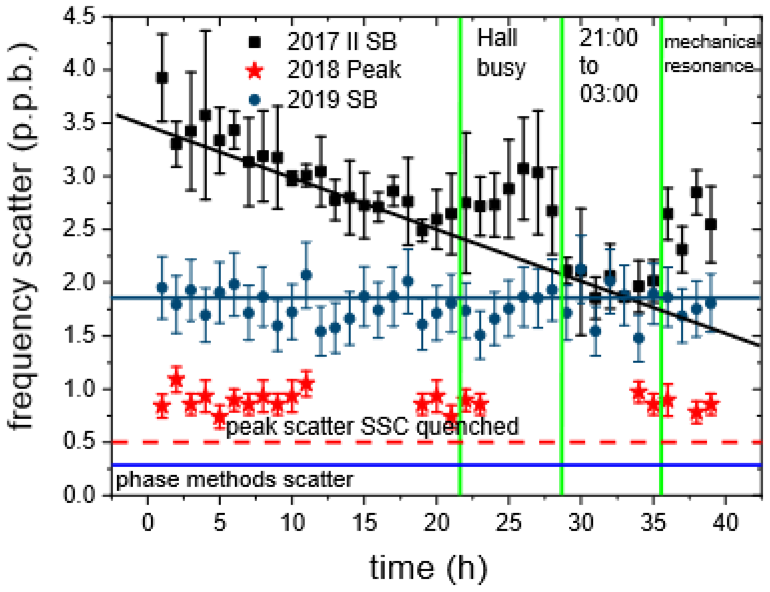

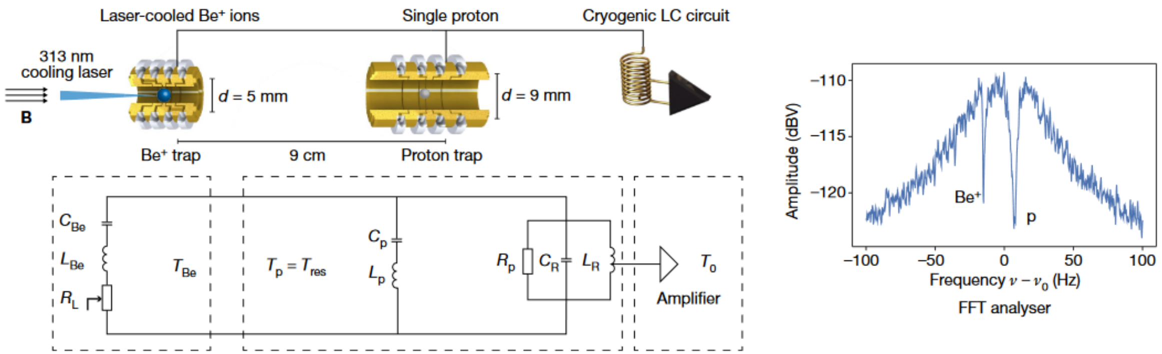

[1] M.J. Borchert, Challenging the Standard Model by high precision comparisons of the fundamental properties of antiprotons and protons, 2021.
[2] M. Bohman *et al.*, Sympathetic cooling of a trapped proton mediated by an LC circuit., *Nature* **596**, 514–518 (2021).
[3] C. Smorra et al., Technical Design Report of BASE-STEP, 2021.

Conclusion and Outlook

- Past measurements were limited by magnetic inhomogeneity and statistics
- New shimming and shielding system removes dominant uncertainty
- Cooling trap increases measurement statistics significantly

→Upgrade experiment for new antiproton energy

→Measure antiproton g-factor to 100 p.p.t. level during the next run


BASE
ETH zürich
RIKEN
MAX-PLANCK-GESELLSCHAFT
CERN
JG|U
JOHANNES GUTENBERG UNIVERSITÄT MAINZ
Leibniz
Universität
Hannover
PTB
GSI
東京大学
DEPART CIRCUIT
VISITES AD

Shimming coil loading scheme

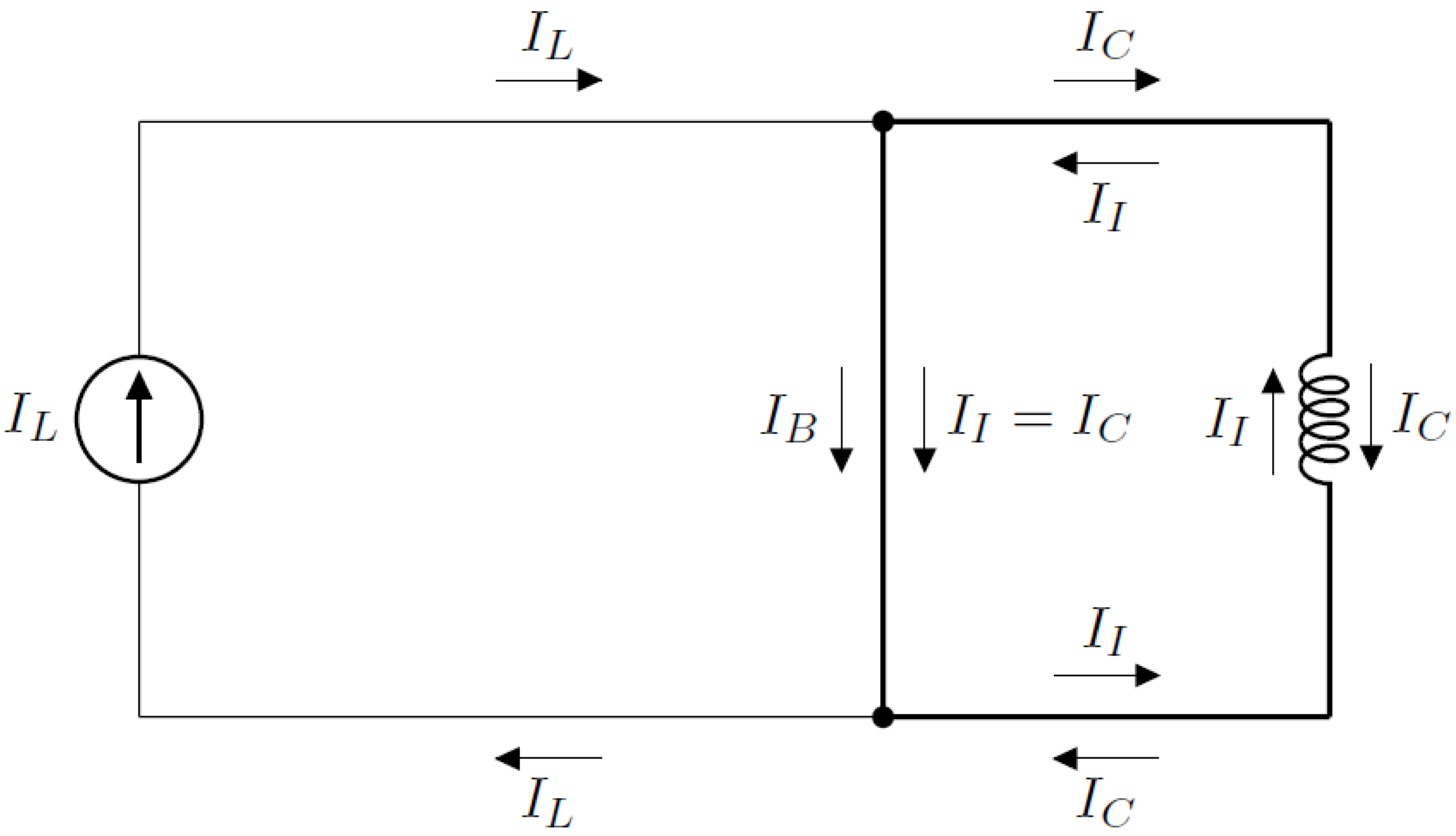

Shimming coil loading scheme

1. Apply quench current

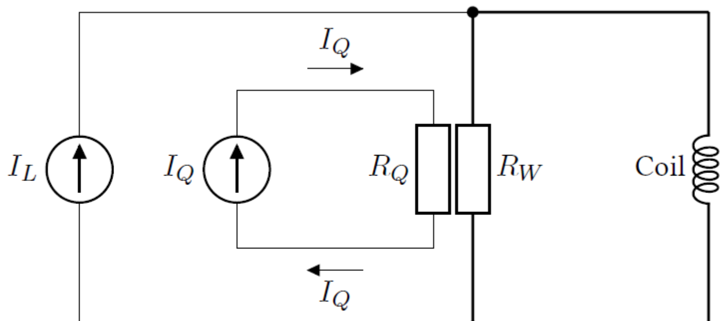

2. Apply loading current

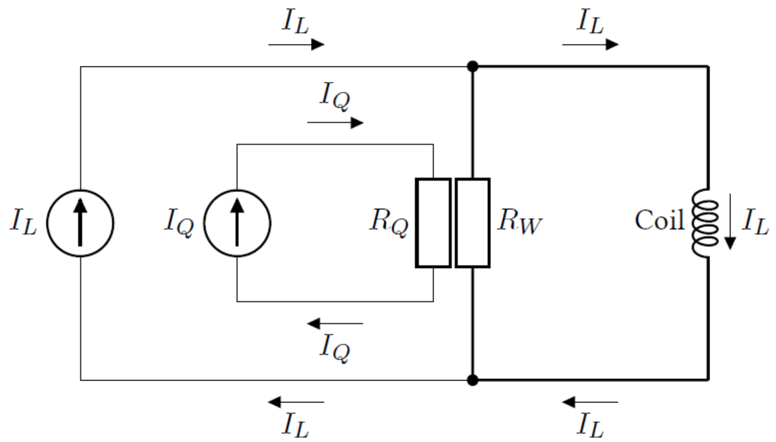

3. Remove quench current

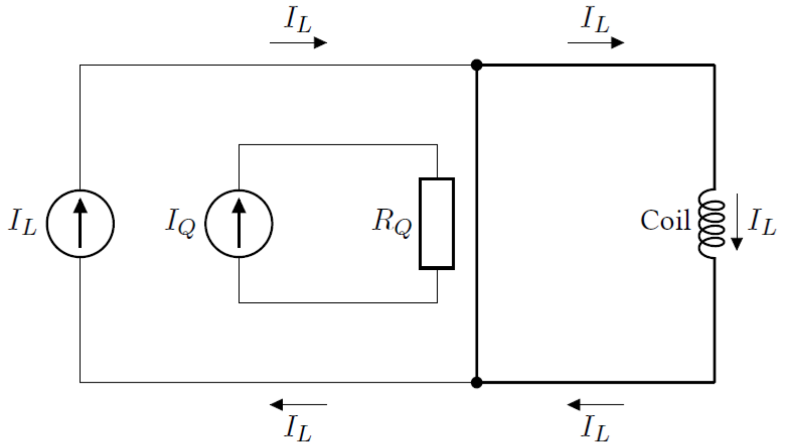

4. Remove loading current

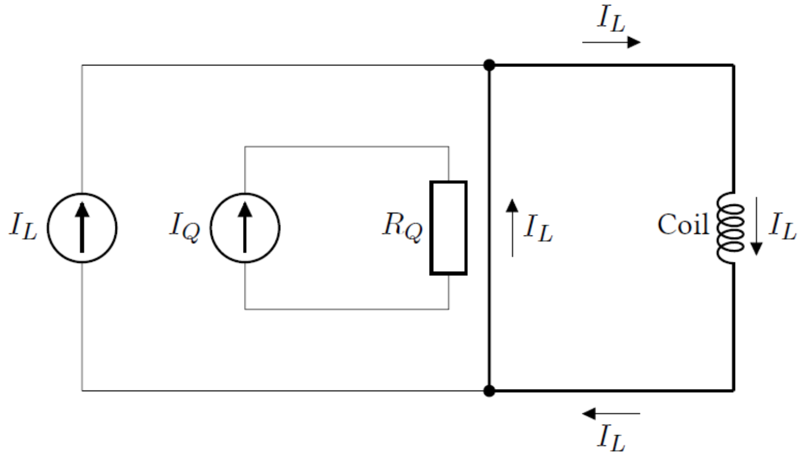

Self-shielding coil

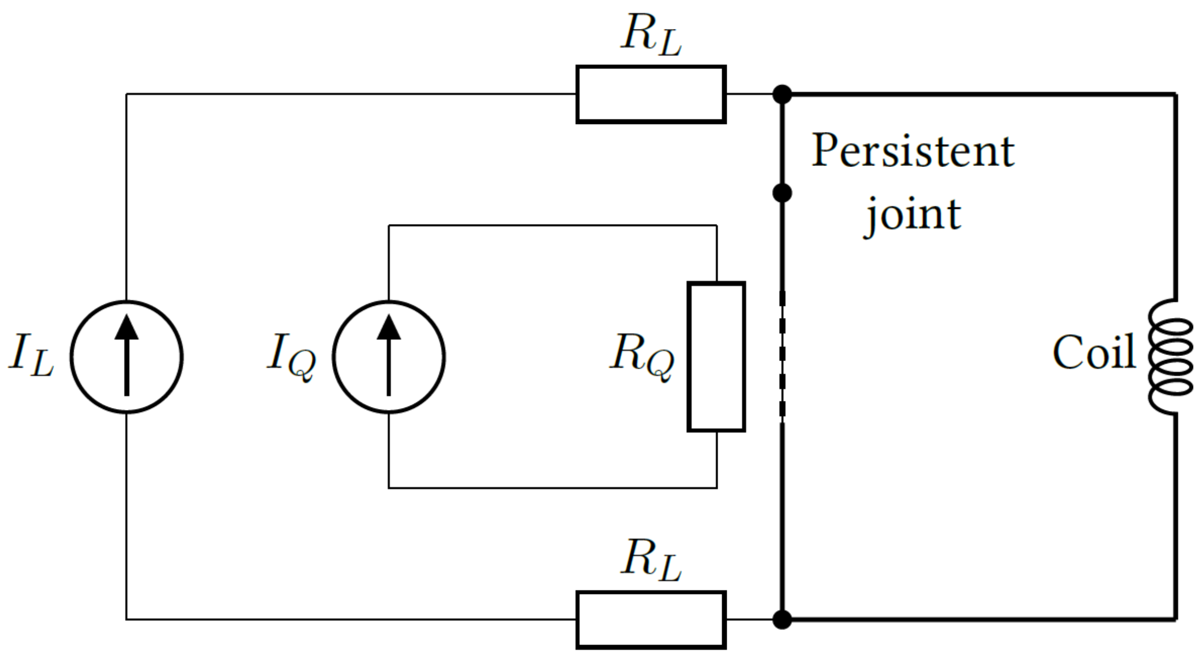

Coil system joints

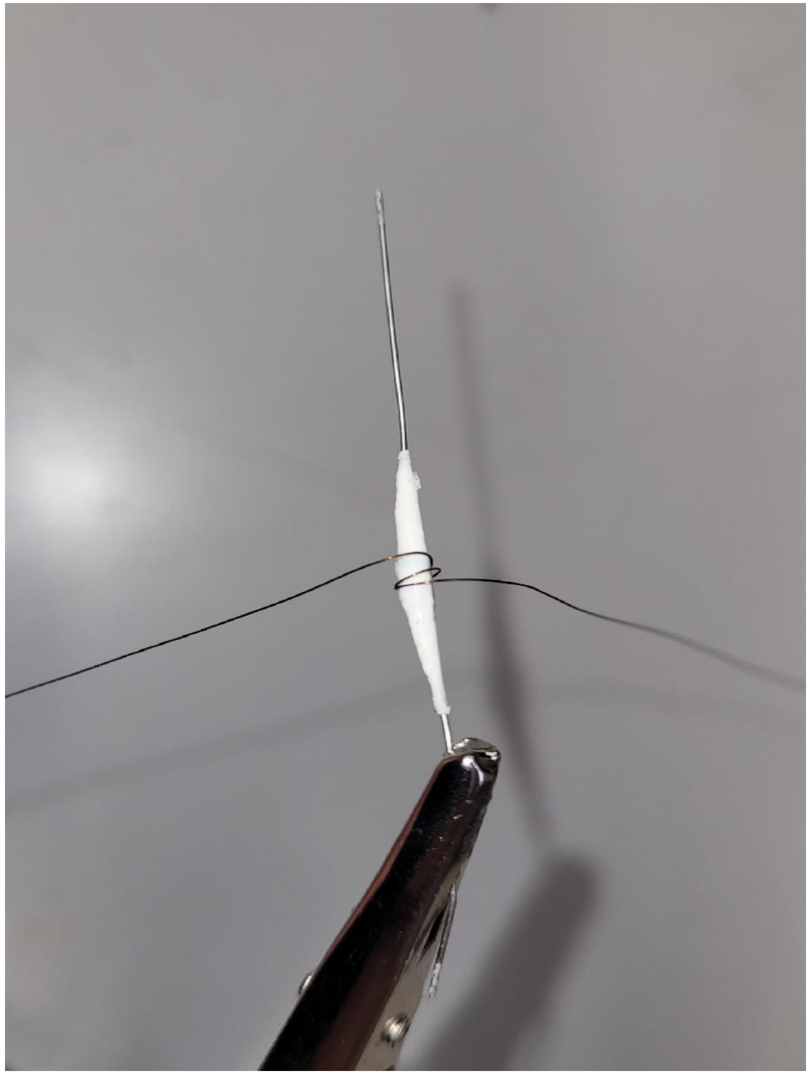

BASE axial field strength

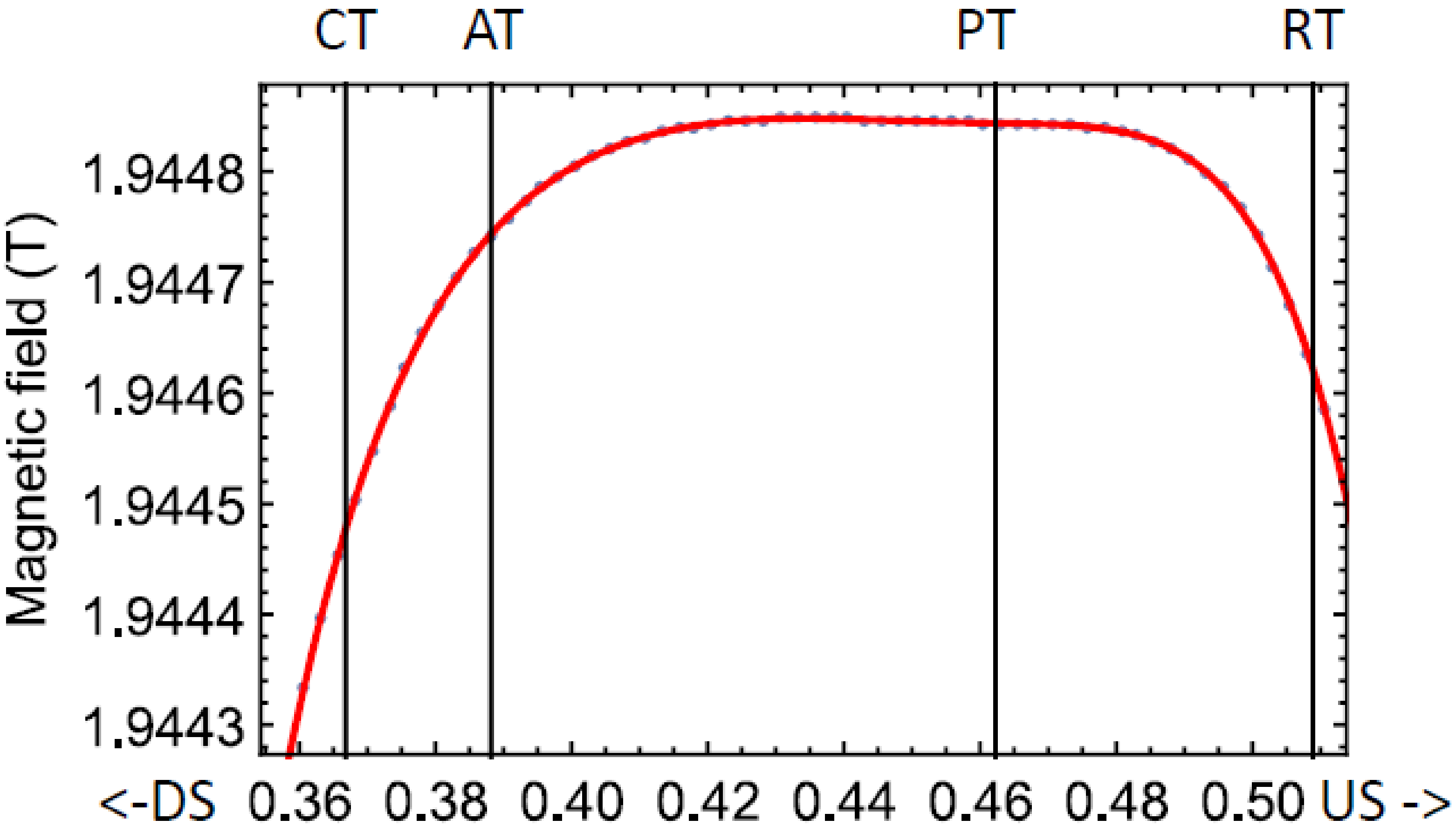

Coil system joints

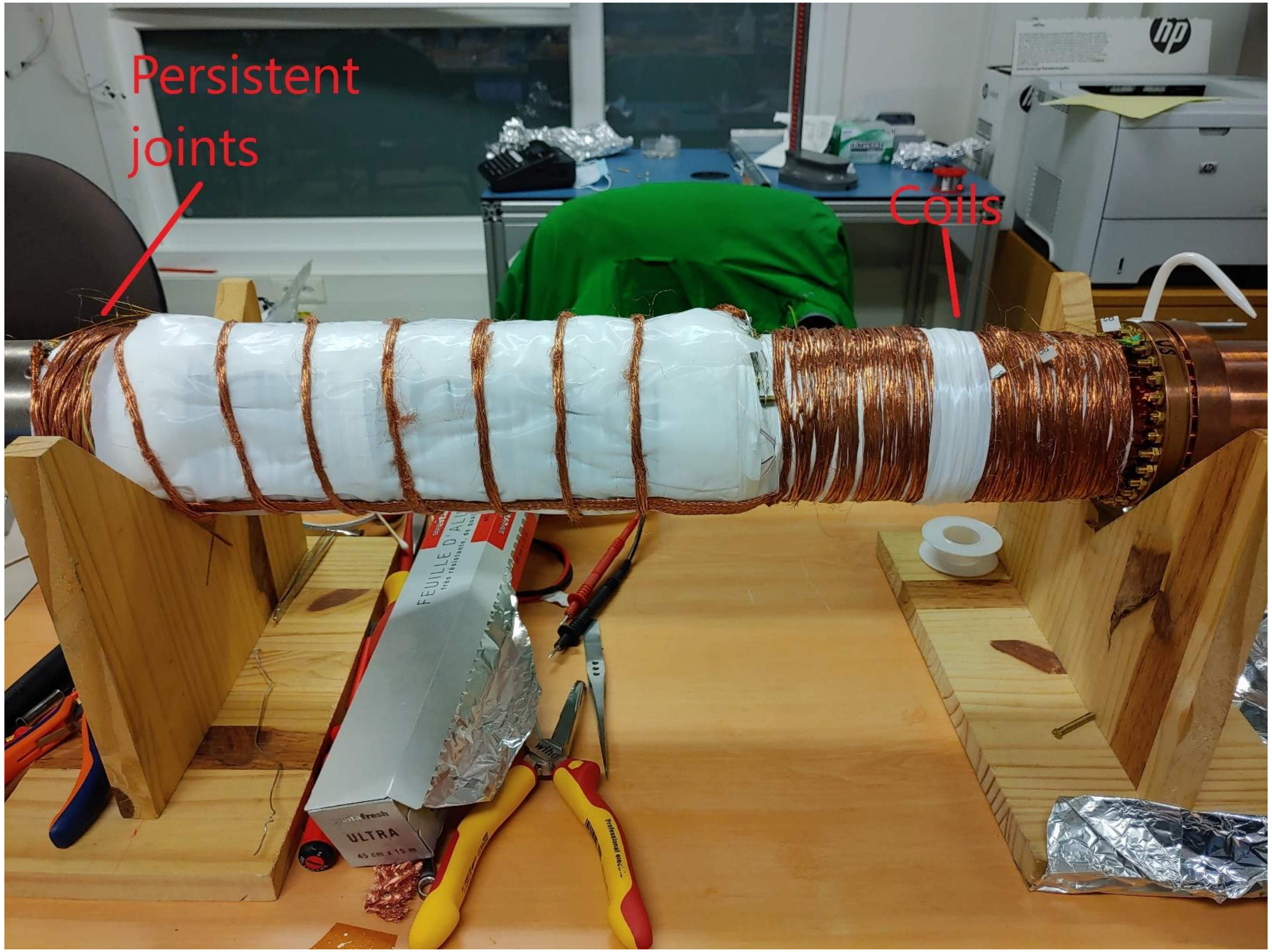

Charge-to-Mass ratio systematics

Effect	2018-1-SB	2018-2-SB	2018-3-PK	2019-1-SB
B_1-shift	0.03(2)	0.01(2)	< (0.01)	< (0.01)
B_2-shift	20.27(14.86)	8.38(14.86)	10.79(12.66)	3.75 (5.16)
C_4-shift	(1.12)	(1.13)	(1.54)	(0.76)
C_6-shift	< (0.01)	< (0.01)	< (0.01)	< (0.01)
Relativistic	1.20(92)	0.47(90)	1.90(2.32)	0.65(94)
Image charge shift	0.05(0)	0.05(0)	0.05(0)	0.05(0)
Trap misalignment	0.06(0)	0.06(0)	0.05(0)	0.05(0)
Voltage Drifts	−3.35(5.12)	−3.77(5.12)	−0.11(11)	−5.03(5.12)
Spectrum Shift	0.37(20.65)	16.89(46.49)	0.74(61)	−8.61(21.45)
FFT-Distortions	(1.57)	(3.48)	(0.03)	(1.23)
Resonator-Shape	0.02(3)	0.02(2)	< (0.01)	0.01(2)
B_1-drift offset	< (0.11)	< (0.11)	< (0.04)	< (0.04)
Resonator Tuning	< (0.16)	< (0.16)	< (0.06)	< (0.06)
Averaging Time	–	–	−2.87(25)	–
FFT Clock	–	–	(3.69)	–
Pulling Shift	–	–	2.86(24)	–
Linear Coefficient Shift	–	–	0.16(40)	–
Nonlinear Shift	–	–	0.03(2)	–
Systematic Shift	18.65(26.04)	22.11(49.22)	13.60(13.50)	−9.13(22.71)
$R_{exp} - R_{theo}$	13.02(27.12)	−5.04(46.57)	7.99(18.57)	18.34(18.89)
$R_{exp,c} - R_{theo}$	−5.63(37.60)	−27.15(67.76)	−5.61(22.66)	27.47(29.54)

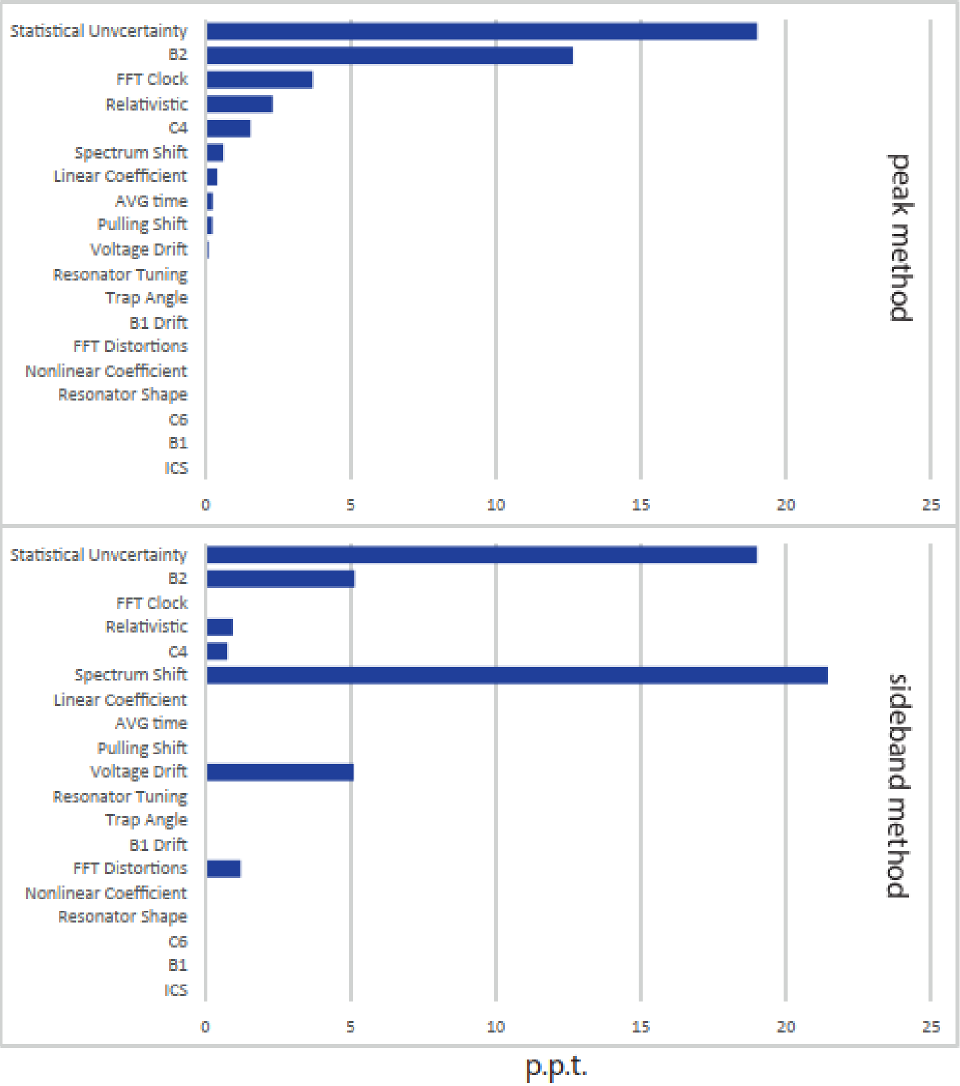

Optimized Larmor resonance

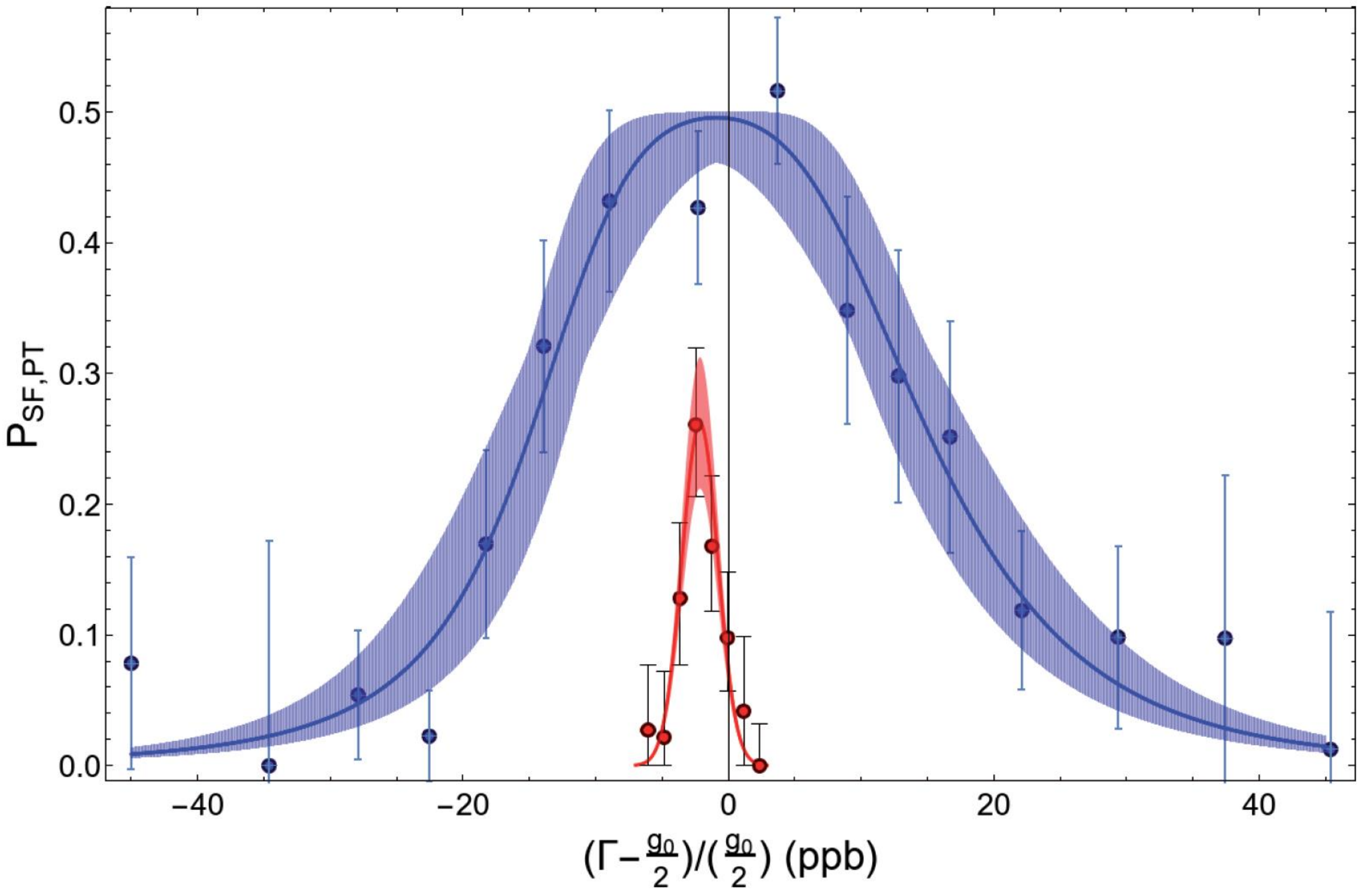

SCHNEIDER, Georg, et al. Double-trap measurement of the proton magnetic moment at 0.3 parts per billion precision. *Science*, 2017, 358. Jg., Nr. 6366, S. 1081-1084.

The cooling trap

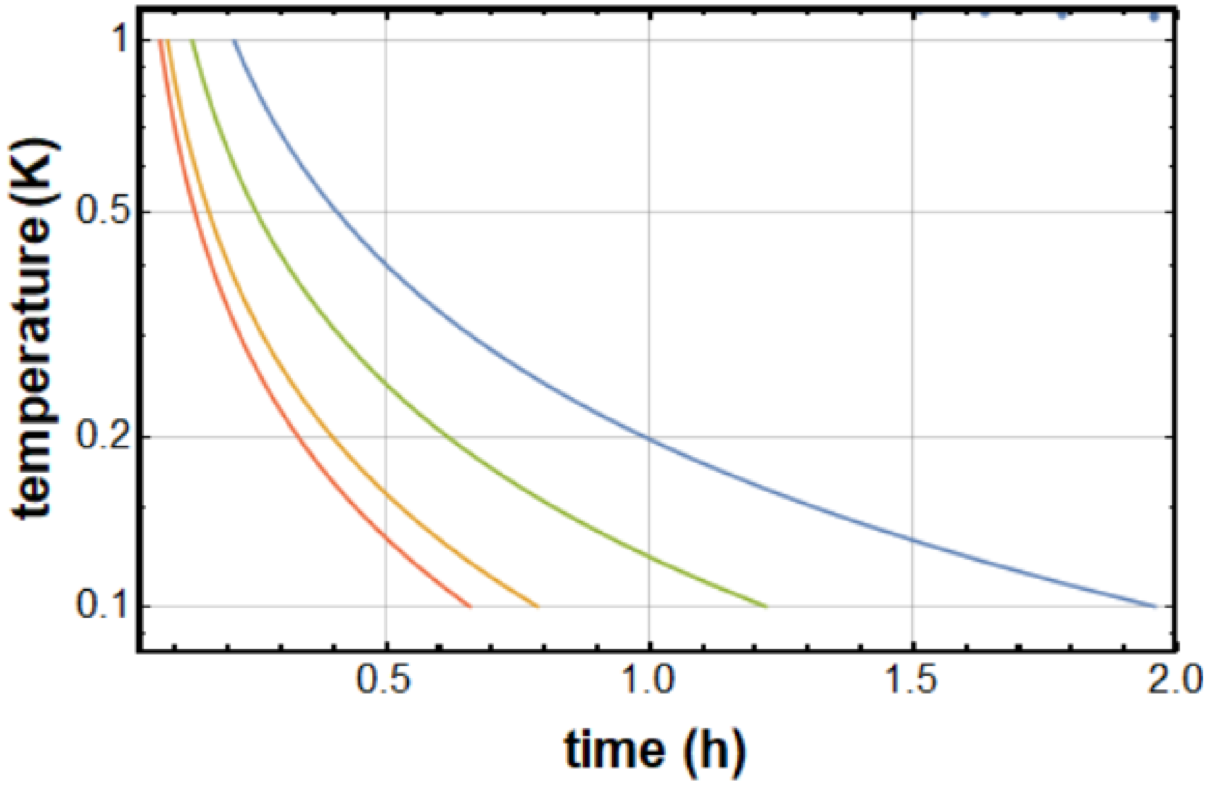

- Status today with 30s cooling in the CT.
- Optimization of spectrum acquisition time (64s to 18s) (should be possible for positive AT feedback).
- Optimization of spectrum acquisition time (64s to 18s) AND CT cooling (30s to 3s).
- Optimization of spectrum acquisition time (64s to 18s) AND CT cooling (30s to 3s) AND further transport optimization.

SME constraints

Coefficient	Limit
$\|\tilde{b}_p^{Z}\|$	$< 1.8 \cdot 10^{-24}$ GeV
$\|\tilde{b}_p^{XX} + \tilde{b}_p^{YY}\|$	$< 1.1 \cdot 10^{-8}$ GeV^{-1}
$\|\tilde{b}_p^{ZZ}\|$	$< 7.8 \cdot 10^{-9}$ GeV^{-1}
$\|\tilde{b}_p^{*Z}\|$	$< 3.5 \cdot 10^{-24}$ GeV
$\|\tilde{b}_p^{*XX} + \tilde{b}_p^{*YY}\|$	$< 7.4 \cdot 10^{-9}$ GeV^{-1}
$\|\tilde{b}_p^{*ZZ}\|$	$< 2.7 \cdot 10^{-8}$ GeV^{-1}

Coefficient	Limit
$\tilde{b}_p^{*X}$	$< 9.7 \cdot 10^{-25}$ GeV
$\tilde{b}_p^{*Y}$	$< 9.7 \cdot 10^{-25}$ GeV
$\|\tilde{b}_p^{*XX} - \tilde{b}_p^{*YY}\|$	$< 5.4 \cdot 10^{-9}$ GeV^{-1}
$\tilde{b}_p^{*XZ}$	$< 3.7 \cdot 10^{-9}$ GeV^{-1}
$\tilde{b}_p^{*YZ}$	$< 3.7 \cdot 10^{-9}$ GeV^{-1}
$\tilde{b}_p^{*XY}$	$< 2.7 \cdot 10^{-9}$ GeV^{-1}

Coefficient	Previous Limit	Improved Limit	Factor
$\|\tilde{c}_e^{XX}\|$	$< 3.23 \cdot 10^{-14}$	$< 7.79 \cdot 10^{-15}$	4.14
$\|\tilde{c}_e^{YY}\|$	$< 3.23 \cdot 10^{-14}$	$< 7.79 \cdot 10^{-15}$	4.14
$\|\tilde{c}_e^{ZZ}\|$	$< 2.14 \cdot 10^{-14}$	$< 4.96 \cdot 10^{-15}$	4.31
$\|\tilde{c}_p^{XX}\|, \|\tilde{c}_p^{*XX}\|$	$< 1.19 \cdot 10^{-10}$	$< 2.86 \cdot 10^{-11}$	4.14
$\|\tilde{c}_p^{YY}\|, \|\tilde{c}_p^{*YY}\|$	$< 1.19 \cdot 10^{-10}$	$< 2.86 \cdot 10^{-11}$	4.14
$\|\tilde{c}_p^{ZZ}\|, \|\tilde{c}_p^{*ZZ}\|$	$< 7.85 \cdot 10^{-11}$	$< 1.82 \cdot 10^{-11}$	4.31

GSHFS Antihydrogen

Deviation from ν_F due to proton structure	$-32.77(1)$ ppm
Recoil corrections	$+5.85(7)$ ppm
Finite electric and magnetic radius (Zemach corrections)	$-41.43(44)$ ppm
Polarizability of proton	$+1.88(64)$ ppm
Remaining deviation theory-experiment	$+0.86(78)$ ppm